Thermal and Quantum Phase Transitions

Lectures given at the
Les Houches Doctoral Training School in Statistical Physics 2015

Matthias Vojta, TU Dresden

October 9, 2015

Contents

Contents **2**

1 Introduction **4**
1.1 Recommended literature 4
1.2 What is a phase? 4
1.3 What is a phase transition? 5
1.4 What is a quantum phase transition? 5

2 Classical phase transitions and universality **7**
2.1 Generic phase diagrams of fluids and magnets 9
2.2 Landau theory 10
2.2.1 Landau functional 10
2.2.2 Ginzburg-Landau theory and spatial correlations 14
2.2.3 Fluctuations and Ginzburg criterion 17
2.3 Critical exponents and universality 18
2.4 Scaling hypothesis 19

3 Renormalization group **21**
3.1 Concept of RG 21
3.2 Scaling transformation and scaling dimension 22
3.3 Momentum-shell RG for the $\mathbb{O}(N)$ ϕ^4 model 23
3.3.1 Fixed points 28
3.3.2 Field renormalization and anomalous exponent 32
3.4 Phase transitions and critical dimensions 33

4 Theoretical models for quantum phase transitions **35**
4.1 Quantum Ising model 35
4.2 Quantum rotor model 37
4.3 Coupled-dimer model 38

5 Quantum phase transitions: Primer **40**
5.1 Classical and quantum fluctuations 40
5.2 Phenomenology: Phase diagrams and crossovers 41

5.3 Quantum ϕ^4 theory . . . 43
5.4 Quantum scaling hypothesis . . . 44
5.5 Quantum-to-classical mapping . . . 46
5.5.1 Classical Ising chain . . . 46
5.5.2 Scaling limit and universality . . . 47
5.5.3 Mapping to a quantum spin . . . 49
5.5.4 Mapping: XY-chain $\leftrightarrow$ $\mathbb{O}(2)$ quantum rotor . . . 50
5.5.5 Mapping: Heisenberg chain $\leftrightarrow$ $\mathbb{O}(3)$ quantum rotor . . . 50
5.5.6 Quantum-to-classical correspondence: Rules and exceptions . . . 50

6 Magnetic quantum phase transitions 52
6.1 Order parameters and response functions . . . 52
6.2 Properties of the quantum ϕ^4 model . . . 54
6.3 Quantum Ising chain . . . 56
6.3.1 Strong-coupling limit $g \gg 1$ . . . 56
6.3.2 Weak-coupling limit $g \ll 1$ . . . 57
6.3.3 Exact spectrum . . . 58
6.3.4 Results near criticality . . . 60

7 Quantum phase transitions of bosons and fermions 63
7.1 Bose-Hubbard model . . . 63
7.2 Bose-Hubbard model: Mean-field theory . . . 64
7.3 Superfluid-insulator transition: Field theory . . . 66
7.3.1 Quadratic vs. linear time derivative . . . 67
7.4 Dilute Bose gas . . . 68
7.5 Dilute spinless Fermi gas . . . 70
7.6 Fermi-Hubbard Model . . . 72
7.6.1 Antiferromagnetism in the Mott insulator . . . 73
7.6.2 Phases of the Hubbard model . . . 74

Bibliography 75

Chapter 1

Introduction

1.1 Recommended literature

- **N. Goldenfeld, Lectures on Phase Transitions and the Renormalization Group**
- **S. Sachdev, Quantum Phase Transitions (2nd ed)**
- S. K. Ma, Modern Theory of Critical Phenomena
- H. E. Stanley, Introduction to Phase Transitions and Critical Phenomena
- P. M. Chaikin, T. C. Lubensky, Principles of Condensed Matter Physics
- J. W. Negele, H. Orland, Quantum Many-Particle Systems
- M. E. Peskin, D. V. Schroeder, An Introduction to Quantum Field Theory
- A. Auerbach, Interacting Electrons and Quantum Magnetism
- K. Yosida, Theory of Magnetism

1.2 What is a phase?

Phase (a definition attempt): Equilibrium state of matter whose qualitative characteristics do not change upon small changes of external parameters (alternatively: which is stable under infinitesimal parameter changes). Within a phase, the thermodynamic potential varies in an analytic fashion.

Phases can be characterized by their symmetries (more precisely: the symmetries of their density operator). Different phases are separated by phase transitions.

1.3 What is a phase transition?

Phase transition: Point in parameter space where the equilibrium properties of a system change qualitatively. The system at a phase transition is unstable w.r.t. infinitesimal changes of external parameters; this implies non-analytic behavior of the thermodynamic potential as function of system parameters.

Thermal phase transitions occur upon varying the temperature. Often, the transition is from an ordered low-temperature phase to a disordered high-temperature phase. Thus, order is destroyed by thermal fluctuations. Phase transitions can be continuous or discontinuous, see Chapter 2.

1.4 What is a quantum phase transition?

Quantum phase transitions (QPT) are phase transitions at temperature $T = 0$ which occur upon varying a non-thermal control parameter (such as pressure, magnetic field, or chemical composition). A QPT implies non-analytic behavior of the ground-state energy as function of the control parameter.

As there are no thermal fluctuations at zero temperature, a QPT is apparently driven by "quantum fluctuations". Note that the term "fluctuations" has to be used with care: At zero temperature, a quantum system is described by a single phase-coherent (many-body) wavefunction. The term "fluctuations" is most appropriately used to characterize

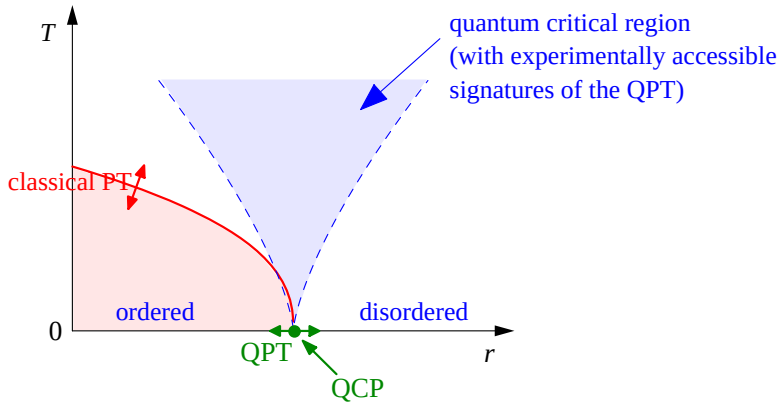

Figure 1.1: Generic phase diagram in the vicinity of a continuous quantum phase transition. The horizontal axis represents the control parameter r used to tune the system through the QPT, the vertical axis is the temperature T. The dashed lines indicate the boundaries of the quantum critical region, located above the quantum critical point (QCP). The solid line marks the finite-temperature boundary between the ordered and disordered phases. Close to this line, the critical behavior is classical.

deviations from a reference state (e.g. an ordered magnet).

Experimentally, zero temperature cannot be accessed. Why are QPT interesting (and more than just an academic curiosity)? To understand this, we have to consider the generic "quantum critical" phase diagram as function of both the non-thermal control parameter and temperature, Fig. 1.1. For a continuous QPT, the zero-temperature axis is divided into two stable phases separated by a quantum critical point (QCP). The finite-T part contains two low-temperature regimes derived from the stable phases and a so-called "quantum critical" regime at elevated temperatures above the QCP.

The stable phases typically display conventional quasiparticle excitations, i.e., objects with conventional quantum numbers (and statistics) which can be identified through sharp peaks in appropriate spectral functions; examples are particle-hole excitations in a Fermi liquid or spin waves in an ordered magnet. In such a situation, the low-temperature thermodynamics can be described as thermal occupation of these quasiparticle states, e.g., leading to a specific heat of $C(T) \propto T$ in a Fermi liquid. In contrast, the elementary excitations of the quantum critical ground state can usually *not* be characterized as quasiparticles, but instead there is a critical continuum of excitations. (Examples will be presented in the course of this lecture.) Now, upon increasing temperature starting from the QCP, this critical continuum will be excited, resulting in power-law behavior of thermodynamic observables as function of temperature with non-trivial exponents. These power laws are the experimentally accessible signatures of quantum criticality; they signal the ground state at the QCP being a "novel state of matter".

Chapter 2

Classical phase transitions and universality

To set the stage, we start by summarizing a few terms and definitions which are useful to characterize phase transitions. In cases where we need to be specific we will use the terminology appropriate for an order-disorder transition of a ferromagnet; the concepts are much more general.

Order parameter (OP): The OP is an observable φ, which is

$$\langle\varphi\rangle \begin{cases} = 0 & \text{in the disordered} \\ \neq 0 & \text{in the ordered} \end{cases} \text{ phase.} \tag{2.1}$$

Here, the brackets $\langle\cdot\rangle$ refer to a thermodynamic average in a suitable Gibbs ensemble and, for quantum systems, to a quantum-mechanical expectation value.

In most cases, the OP is chosen to be a *local* observable where "local" means that φ can be (in principle) defined at every point in space and time. Starting from a microscopic description, such a definition may require appropriate coarse-graining, i.e., a suitable average over a larger (i.e. mesoscopic) number of microscopic constituents. (Counter-example: The volume enclosed by the Fermi surface of a metal is not a local observable.)

For the ferromagnet the natural order parameter is the local magnetization. In general, the choice of an order parameter is not unique, and in some cases a suitable order parameter is not even known (e.g. for the interaction-driven metal-to-insulator transition).

First-order transition: The OP changes discontinuously at the transition.

Continuous transition: The OP varies continuously across the transition.

Critical point: The transition point of a continuous transition.

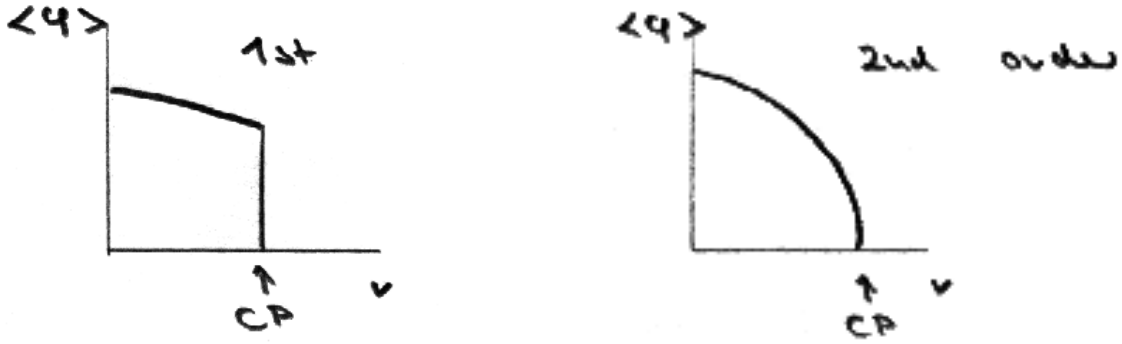

Figure 2.1: Discontinuous and continuous behavior of the order parameter as function of a control parameter r for a first-order and continuous phase transitions, respectively.

Correlations: For an order parameter depending on space and time, $\varphi = \varphi(\vec{r}, t)$, correlation functions can be defined by $\langle \varphi(\vec{r}, t)\varphi(\vec{r}', t')\rangle$.

Correlation length ξ: In stable phases the order-parameter correlation function typically follows an exponential law $\langle \varphi(\vec{r})\varphi(\vec{r}')\rangle - \langle \varphi(\vec{r})\rangle\langle \varphi(\vec{r}')\rangle \propto e^{\frac{|\vec{r}-\vec{r}'|}{\xi}}$, with a correlation length ξ.

Upon approaching a critical point this correlation length ξ diverges, such that $\xi = \infty$ at criticality where the exponential decay with distance is replaced by a power-law decay (recall that power laws are scale-invariant). Near criticality, the correlation length is the only length scale characterizing the low-energy physics.

Spontaneous symmetry breaking: Consider a system, described by the Hamiltonian $\hat{H}$, and a symmetry operation $\hat{S}$, with $\hat{H}$ being symmetric under $\hat{S}$: $[\hat{H}, \hat{S}]_- = 0$. If the system's density operator $\hat{\rho}$ is not symmetric under $\hat{S}$, $[\hat{\rho}, \hat{S}]_- \neq 0$, then the symmetry $\hat{S}$ is spontaneously broken.

To allow for symmetry breaking in Gibbs ensembles (where $[\hat{H}, \hat{S}]_- = 0$ implies $[e^{-\beta\hat{H}}, \hat{S}]_- = 0$) it is necessary to include a (small) field conjugate to the order parameter: $\hat{H} \to \hat{H} - h\varphi$. Then, spontaneous symmetry breaking is equivalent to the limit $h \to 0$ being singular: $\lim_{h\to 0} \hat{\rho}(h) \neq \hat{\rho}(h = 0)$.

Symmetry breaking requires the thermodynamic limit, $N \to \infty$, as a finite-size system cannot show a finite-temperature phase transition ($e^{-\beta\hat{H}}$ being a product of a *finite* number of exponentials cannot be singular). Consequently, spontaneous symmetry breaking is equivalent to the non-commutativity of two limits: $\lim_{h\to 0} \lim_{N\to\infty} \ldots \neq \lim_{N\to\infty} \lim_{h\to 0} \ldots$

2.1 Generic phase diagrams of fluids and magnets

Fig. 2.2 illustrates the phase diagrams of systems near critical points, showing similarities and differences between (a) a fluid which in particular displays a liquid–gas transition and (b) a magnet which displays ferromagnet–paramagnet transition. One key difference is that both the line of first-order transitions and the critical endpoint have enhanced symmetry in the magnetic case, but not in the fluid case. Many aspects of these phase diagrams will be discussed in more detail below.

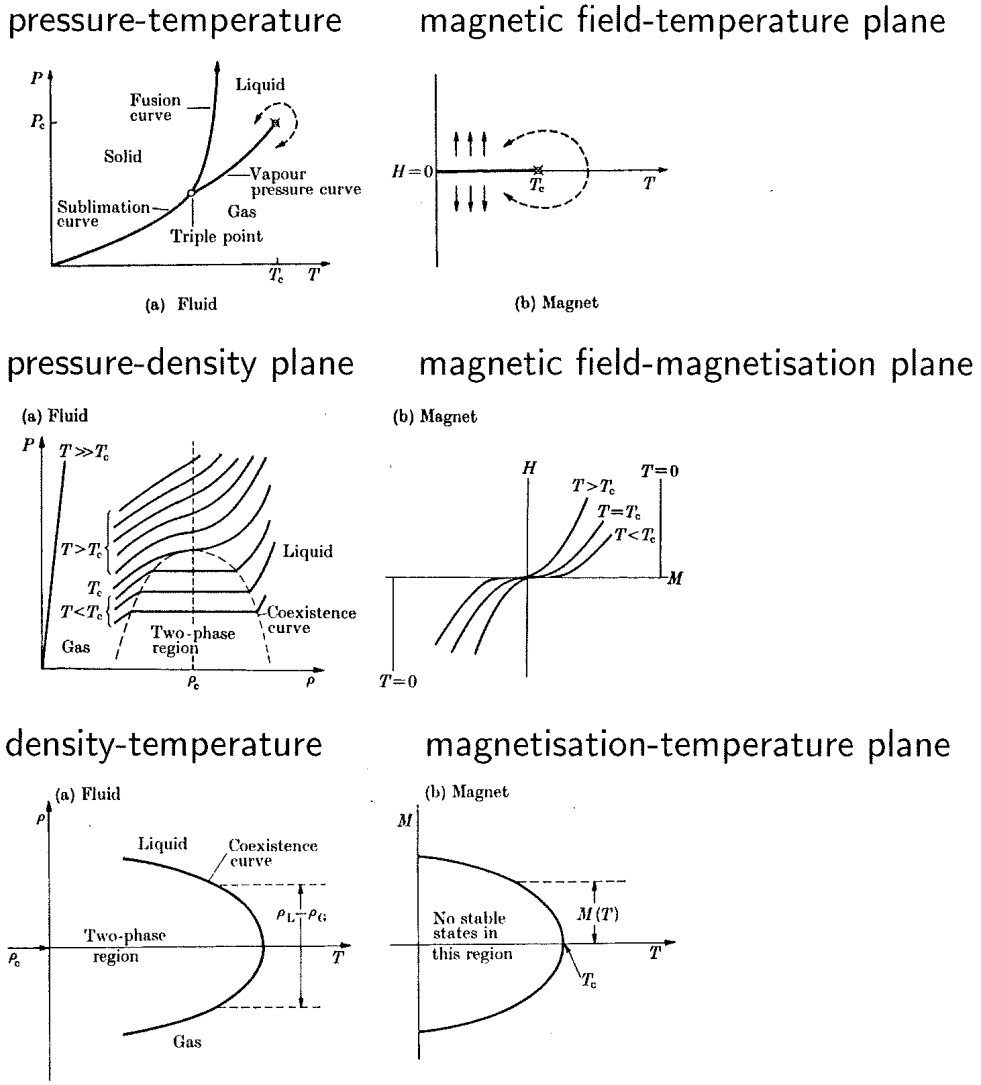

Figure 2.2: Different representations of the generic phase diagrams of (a) fluids and (b) magnets.

2.2 Landau theory

We continue with a brief summary of Landau's theory of phase transitions. Landau theory is based on the concept of a local order parameter φ, which is assumed to be small – the latter assumption is justified near critical points. The goal is to derive thermodynamic properties near phase transitions. A major obstacle in simple calculations is that the thermodynamic potential and its derivatives are non-analytic (as function of external parameters) at the critical point, i.e., no Taylor expansion is possible. In Landau theory, this problem is circumvented by considering a generalized potential which includes an explicit dependence on the order parameter itself.

2.2.1 Landau functional

Landau's approach starts by introducing a generalized thermodynamic potential f, which depends not only on the external variables (of the considered ensemble), but also on the order parameter. Consider e.g. a ferromagnet (FM): In equilibrium, specifying the external magnetic field H and the temperature T fixes the magnetization $\varphi \equiv M$. Landau's approach implies to generalize the equilibrium potential $f(T, H)$ to $f(T, H, \varphi)$. Subsequently, it is assumed that $f(T, H, \varphi)$ is non-singular as function of the order parameter φ. Further, it is postulated that the equilibrium state of the system is given by $\frac{\partial f(T,H,\varphi)}{\partial \varphi} = 0$ which defines φ_{eq}. The (conventional) thermodynamic potential follows as $f(T, H) = f(T, H, \varphi_{\text{eq}}(T, H))$.

In general, the form of $f(T, H, \varphi)$ is not known. However, near criticality where φ is small, we can expand – based on the assumption of analyticity – $f(T, H, \varphi)$ in a Taylor series in φ:

$$f = f_n + f_0 \left(\frac{a}{2}\varphi^2 + \frac{b}{4}\varphi^4 + \frac{c}{6}\varphi^6 + \cdots - \varphi h \right) \tag{2.2}$$

where $h = \frac{H}{f_0}$ is the external field that couples to (or "is conjugate to") the order parameter, and f_n is a weakly T-dependent term which can usually be ignored.

The above expansion keeps all *symmetry-allowed* terms: In the absence of a field, the potential should be independent of the sign of φ – reflecting an underlying $\mathbb{Z}_2$ (or Ising) symmetry $\varphi \leftrightarrow (-\varphi)$ – this forbids odd powers of φ. For a vector order parameter $\vec{\varphi}$ with underlying $\mathbb{O}(N)$ symmetry, all terms should be invariant under $\mathbb{O}(N)$ rotations, such that $\vec{\varphi}^2 = \vec{\varphi} \cdot \vec{\varphi}$, $(\vec{\varphi}^2)^2$, $(\vec{\varphi}^2)^3$ etc. are allowed.

As Eq. (2.2) represents an effective model for the order parameter, its coefficients a, b, ... can be assumed to be smooth functions of those external parameters which preserve the symmetries of the problem (in particular, of the temperature).

Discussion for $h = 0$ for the expansion up to 4th order: The minima of the potential f (see Fig. 2.3) as a function of φ is determined by $\frac{\partial f}{\partial \varphi} = 0$ and they are given

by

$$\varphi = \begin{cases} 0 & a > 0 \quad \text{disordered state} \\ \pm\sqrt{-a/b} & a < 0 \quad \text{ordered state} \end{cases} \tag{2.3}$$

where $b > 0$ is required by stability (otherwise f would be unbounded from below, and $|\varphi|$ would tend to infinity). Note that $\varphi = 0$ is also a solution of $\frac{\partial f}{\partial \varphi} = 0$ for $a < 0$, but here it corresponds to a maximum of f, to be interpreted as an unstable state.

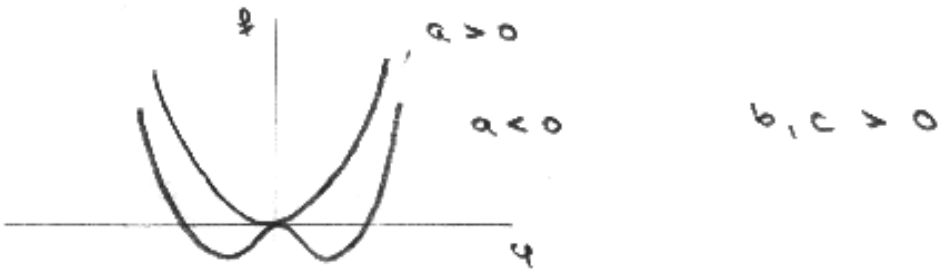

Figure 2.3: Functional dependence of the Landau potential f (2.2) on the order parameter φ for $h = 0$.

Apparently, $a = 0$ corresponds to the phase transition point, $T = T_c$. As a should be a smooth function of temperature, we can expand to lowest non-vanishing order $a(T) = \alpha(T - T_c)/T_c \equiv \alpha t$ where we have introduced the *reduced temperature*

$$t = \frac{T - T_c}{T_c} \,. \tag{2.4}$$

The order parameter is then given by

$$\varphi = \begin{cases} 0 & T > T_c \\ \pm\sqrt{\dfrac{\alpha}{b}(-t)} & T < T_c \end{cases} \tag{2.5}$$

This square-root behaviour is characteristic of Landau theory. The two possible signs correspond to spontaneous breaking of the assumed $\mathbb{Z}_2$ symmetry; for a vector order parameter its magnitude would be fixed by $\sqrt{-a/b}$ with its direction being arbitrary.

Thermodynamic observables follow from inserting φ into the expression for the Lan-

dau functional and taking appropriate derivatives:

$$f(T) = \begin{cases} f_n(T) & \text{for } T > T_c \\ f_n(T) - f_0 \frac{\alpha^2}{4b} \left(\frac{T_c - T}{T_c}\right)^2 & \text{for } T < T_c \end{cases}$$

$$S/V = -\frac{\partial f}{\partial T} = \begin{cases} s_0(T) & \text{for } T > T_c \\ s_0(T) - f_0 \frac{\alpha^2}{2b} \frac{T_c - T}{T_c^2} & \text{for } T < T_c \end{cases}$$

$$c = T\frac{\partial (S/V)}{\partial T} = \begin{cases} c_0 & \text{for } T > T_c \\ c_0 + f_0 \frac{\alpha^2}{2b} \frac{1}{T_c} & \text{for } T < T_c \end{cases}$$

The results for entropy and specific heat are schematically shown in Fig. 2.4. In particular, within Landau theory the specific heat displays a jump at T_c (not a power-law singularity).

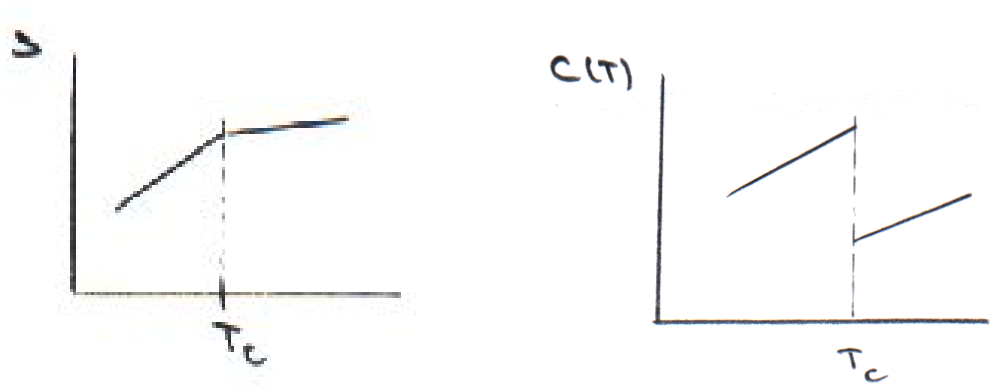

Figure 2.4: Landau-theory results for entropy and specific heat near the transition temperature T_c.

Discussion for $h \neq 0$: Minimizing f with respect to φ yields the equation

$$\alpha t \varphi + b\varphi^3 = h\,. \tag{2.6}$$

For $t > 0$ there is one solution, whereas $t < 0$ yields three solutions for small h (one again corresponding to a maximum of f) and a single solution for large h. The interpretation is obvious, see Fig. 2.5: There is a global minimum of f for one sign of φ (depending on the sign of h), and possibly a local (i.e. metastable) minimum for the other sign of φ. For the ferromagnet, this reflects the fact that the field selects the state with spins parallel to the field.

It is useful to define $\varphi(h) = \varphi_{\mathsf{spont}} + \chi(T) \cdot h$, with $\chi := \left.\frac{\partial \varphi}{\partial h}\right|_{h \to 0}$ being the order-parameter susceptibility and φ_{spont} being the zero-field value of the order parameter

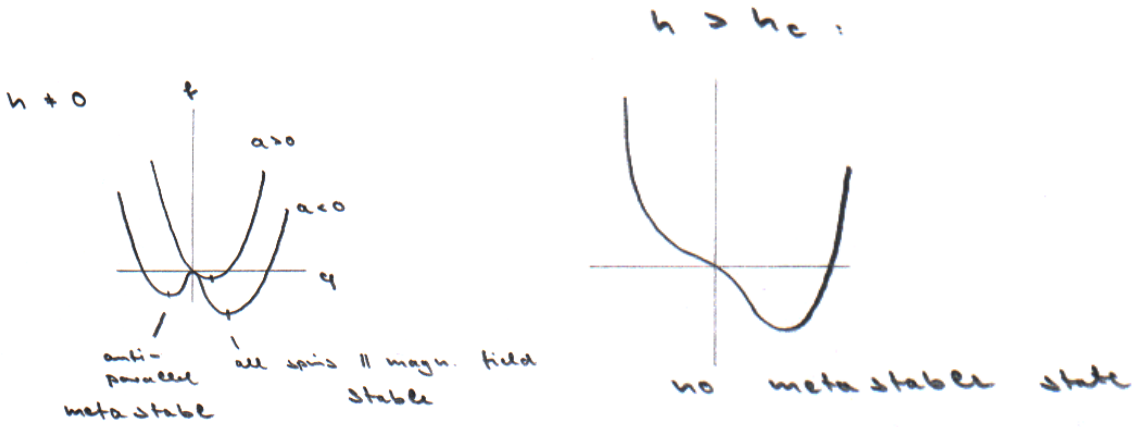

Figure 2.5: Landau potential f (2.2) for $h \neq 0$, displaying minima which correspond to either stable or metastable states.

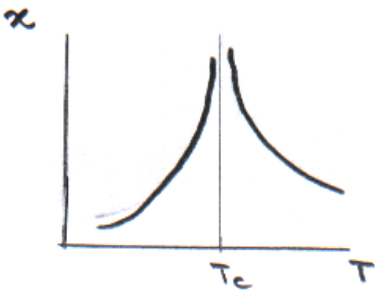

Figure 2.6: Singular behavior of the order-parameter susceptibility χ near T_C. For ferromagnets, the behavior for $T > T_C$, $\chi = C/(T - T_C)$ with C the Curie constant, is also known as Curie-Weiss law.

from Eq. (2.5). The calculation yields the susceptibility χ to be

$$\chi(T) = \begin{cases} \dfrac{1}{t} & T > T_c \\ \dfrac{1}{2|t|} & T < T_c \end{cases} . \tag{2.7}$$

Hence, χ grows upon approaching the transition, and is infinite at T_c, see Fig. 2.6.

At T_c the φ^2 term is absent in f, yielding the field dependence of the order parameter along the critical isotherm,

$$\varphi \propto h^{1/3} , \tag{2.8}$$

see Fig. 2.7. (The general definition is $h \propto |\varphi|^\delta$, here $\delta = 3$.) In the language of a ferromagnet, this singular behavior reflects the fact that, at criticality, it is very easy to polarize the spins.

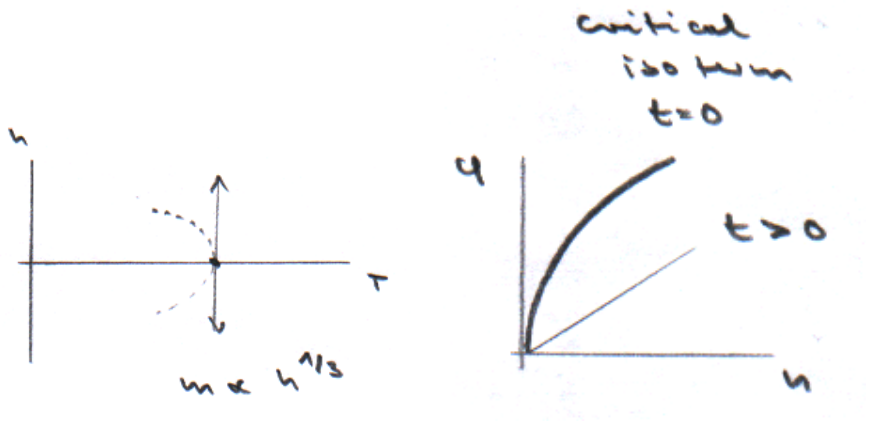

Figure 2.7: Location of the critical isotherm and corresponding order-parameter behavior.

Analysing the phase diagram

- Fig. 2.8 shows that there is a line of first-order phase transitions for $T < T_C$ at $h = 0$ (i.e. from $h < 0$ to $h > 0$). This is a special case of a first-order PT since the two phases are related by symmetry, so there is no latent heat in the transition. (In general, the two phases on both sides of a first-order transition are not symmetry-related, like for the liquid–gas transition, resulting in latent heat given by the entropy difference $Q = \Delta S$.)

- For $T < T_C$ and small h there is a coexistence region where we have two minima of f, the stable and the metastable minimum. The metastable phase can be accessed experimentally in a non-equilibrium setting: if h is varied with a finite rate through $h = 0$, the system switches from the metastable to the stable phase in a delayed fashion, leading to hysteresis.

- For larger h the metastable solution disappears, this marks the end of the coexistence region.

- The continuous temperature-driven PT occurs at T_c at $h = 0$ in Fig. 2.8. In contrast, for $h \neq 0$ there is no PT upon varying the temperature, because the symmetry is already broken by nonzero h.

2.2.2 Ginzburg-Landau theory and spatial correlations

Up to now the order parameter has been assumed to be spatially homogeneous. This assumption can be relaxed, by introducing a spatially varying order-parameter field:

$$\varphi \to \varphi(\vec{r}) \,. \tag{2.9}$$

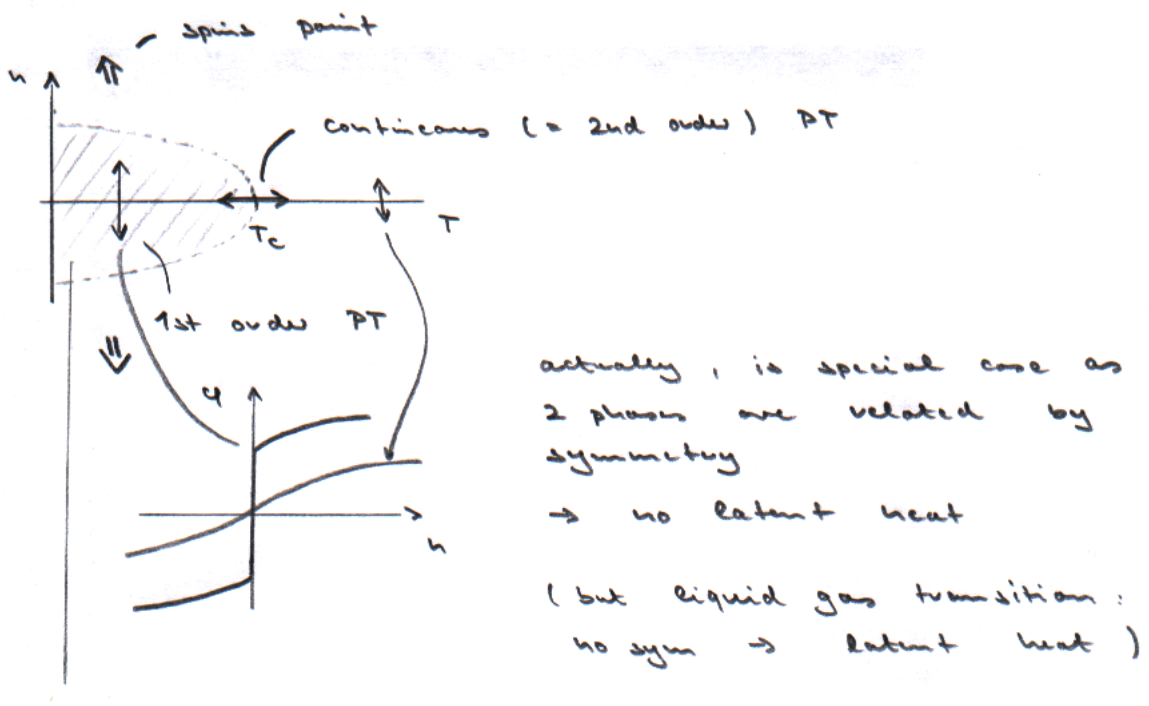

Figure 2.8: Continuous and first-order transitions in the temperature–field phase diagram of a magnet as described by Landau theory.

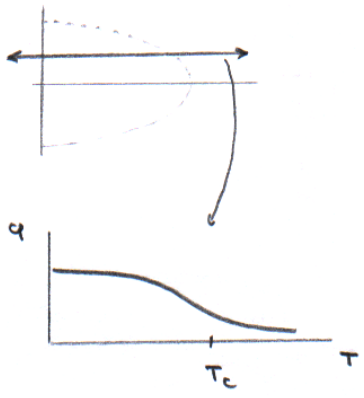

Figure 2.9: Varying the temperature in the presence of a finite field results in a smooth variation of the order parameter.

Here, $\vec{r}$ is a continuous space coordinate. Such a continuum-limit description requires appropriate coarse-graining of microscopic degrees of freedom, as noted above. This also implies that, conceptually, $\varphi(\vec{r})$ should be a smooth function of $\vec{r}$ which captures spatial variations on length scales much larger than microscopic lengths. Such variations can be expected to come with an energy cost, such that the Landau functional generalizes to

$$f(T, H, \varphi(\vec{r})) = f_n + f_0 \left(\frac{a}{2}\varphi(\vec{r})^2 + \frac{b}{4}\varphi(\vec{r})^4 + \xi_0^2 (\vec{\nabla}_{\vec{r}}\varphi(\vec{r}))^2 - \varphi(\vec{r})h \right) \tag{2.10}$$

corresponding to *Ginzburg-Landau theory*. The gradient term can be understood as the lowest additional term arising from an expansion in powers and gradients of φ which is allowed by symmetry: Spatial inversion symmetry forbids odd powers of gradients. Importantly, $f(T, H, \varphi(\vec{r}))$ is a local energy density, and the Ginzburg-Landau (free) energy is

$$F = \int d^d r f(\vec{r})\,. \tag{2.11}$$

Ginzburg-Landau theory has been particularly used in the field of superconductivity, where a complex scalar field φ describes the superconducting condensate which can become inhomogeneous in the presence of an external magnetic field (leading to vortex states).

Using Ginzburg-Landau theory one can also calculate spatial correlations of the OP φ. These are measured by the correlation function

$$G(\vec{r}, \vec{r}\,') = \langle \varphi(\vec{r})\varphi(\vec{r}\,') \rangle - \langle \varphi(\vec{r}) \rangle \langle \varphi(\vec{r}\,') \rangle = \langle \varphi(\vec{r})\varphi(\vec{r}\,') \rangle - \varphi_0^2 \tag{2.12}$$

where φ_0 refers to the spatially homogeneous equilibrium value of φ. Note that in the ordered phase, where $\varphi_0 \neq 0$, we have

$$\lim_{|\vec{r}-\vec{r}\,'|\to\infty} \langle \varphi(\vec{r})\varphi(\vec{r}\,') \rangle = \varphi_0^2 \tag{2.13}$$

reflecting long-range order, and $G(\vec{r}, \vec{r}\,')$ measures correlations of fluctuations around φ_0.

We now sketch the calculation of $G(r)$, for details see e.g. the book of Goldenfeld [2]. A deviation $\delta\varphi$ of the order parameter from its equilibrium value φ_0 increases the free energy by

$$\delta F = \frac{f_0}{2} \int d^d r \; \delta\varphi(\vec{r}) \left(\alpha t + 3b\varphi_0^2 - \xi_0^2 \vec{\nabla}_{\vec{r}}^2 \right) \delta\varphi(\vec{r}) \tag{2.14}$$

After a Fourier decomposition of $\delta\varphi$ the correlation function can be calculated as expectation value weighted by $\exp(-\beta\delta F)$. The result is

$$G(k) = \langle \delta\varphi(\vec{k})\delta\varphi(-\vec{k}) \rangle = \frac{kT}{f_0(A + \xi_0^2 k^2)} \tag{2.15}$$

where $A = \alpha t + 3b\varphi_0^2$. Fourier-transforming back to real space yields $G(r)$. For large $r = |\vec{r} - \vec{r}\,'|$ the correlation function has the limit

$$G(r) \propto \frac{e^{-r/\xi(T)}}{r^{(d-1)/2}} \xi^{(3-d)/2} \tag{2.16}$$

which is dominated by the exponential at large distances. The so defined correlation length depends in Ginzburg-Landau theory on the reduced temperature t as

$$\xi(T) = \begin{cases} \xi_0/\sqrt{\alpha t} & T > T_C \\ \xi_0/\sqrt{2\alpha|t|} & T < T_C \end{cases} \tag{2.17}$$

The divergence of ξ is then $\xi \propto |t|^{-\nu}$, $\nu = \frac{1}{2}$. A diverging correlation length implies that, as we approach the critical point, there are locally ordered islands of increasing size. The fact that, near criticality, the order parameter varies slowly in space is an a-posteriori justification of the gradient expansion in Ginzburg-Landau theory.

As will be discussed later, the diverging correlation length is accompanied by a diverging correlation time, i.e., the fluctuations of these island become slower and slower upon approaching criticality – a phenomenon known as critical slowing down.

Using the Ginzburg-Landau result (2.15), we find that the correlation function at the critical point decays in a power-law fashion:

$$G(r) \propto r^{2-d} \qquad (\xi = \infty) \tag{2.18}$$

Note that this result can obviously only apply to $d > 2$.

2.2.3 Fluctuations and Ginzburg criterion

So far, we have described Landau theory as a simple phenomenological theory describing a phase transition, which can be applied to systems with one (or more) local order parameters. As will become clear later, Landau theory can be interpreted as the saddle-point solution to a more general theory (formulated in the path-integral language) where the order-parameter field φ is allowed to fluctuate in space and time. As the saddle-point solution fixes φ, its fluctuations are neglected in Landau theory. This is a serious (mean-field-type) approximation.

We can assess the validity of the neglect of fluctuations using a simple estimate based on Landau theory itself:

$$\frac{\langle\, \delta\varphi(\,\vec{r} = \xi(T)\,)\;\delta\varphi(\,\vec{r} = 0\,)\,\rangle}{\varphi_0^2} \overset{\langle\delta\varphi(\xi)\,\delta\varphi(0)\rangle \propto \xi^{2-d}}{\underset{\varphi_0 \propto (-t)^{1/2}}{\overset{\downarrow}{\propto}\uparrow}} \frac{\xi(T)^{2-d}}{|t|} \overset{\xi \propto |t|^{-1/2}}{\propto} |t|^{\frac{d-4}{2}} \xrightarrow[|t|\to 0]{} \begin{cases} 0 & d > 4 \\ \infty & d < 4 \end{cases} \tag{2.19}$$

This estimate, known as Ginzburg criterion, shows that fluctuations become inevitably important upon approaching criticality in dimensions $d < 4$, whereas they are unimportant for $d > 4$. This implies that Landau theory is asymptotically exact for $d > 4$, in particular the critical exponents predicted by Landau theory (often dubbed mean-field exponents) are exact for $d > 4$. In contrast, for $d < 4$ fluctuations cannot be neglected close to criticality, and hence Landau theory fails. $d_c^+ = 4$ is called upper critical dimension.

Two remarks are in order: (i) It is interesting to see that Landau theory can predict its own failure (many other approximate theories don't). (ii) There are systems in $d = 3$ where mean-field exponents can be observed experimentally: This happens if the numerical prefactor in front of relevant fluctuation terms is small. The Ginzburg criterion remains valid, but applies only to the immediate vicinity of the critical point which may be experimentally inaccessible. One important example is the superconducting transition of conventional superconductors in $d = 3$: Here fluctuations become important only if $t < 10^{-10}$ or so, due to the small ratio of transition temperature and Fermi temperature.

2.3 Critical exponents and universality

As we have seen above, the critical point is characterized by a diverging correlation length: $\xi \to \infty$. This implies that the order-parameter fluctuations do not display a characteristic length scale at criticality, hence fluctuations exist on all length scales. The system is said to be scale-invariant, i.e., looks "similar" on all length scales.

A consequence of scale invariance is that observables depend on parameters (like t h etc.) in the form of power laws, because power laws $A \sim x^\alpha$ are the only scale-invariant dependencies. These power laws define *critical exponents* and are an important part of critical phenomena. Commonly used critical exponents are given in Table 2.1, together with their mean-field values (as obtained from Ginzburg-Landau theory).

Table 2.1: Table of critical exponents

	Exp.	Definition	Conditions	MF value (GL)
Specific heat	α	$C \propto \lvert t\rvert^{-\alpha}$	$t \to 0, h = 0$	$\alpha = 0$
Order parameter	β	$\varphi \propto (-t)^\beta$	$t \to 0^-, h = 0$	$\beta = \frac{1}{2}$
Susceptibility	γ	$\chi \propto \lvert t\rvert^{-\gamma}$	$t \to 0, h = 0$	$\gamma = 1$
Critical isotherm	δ	$h \propto \lvert\varphi\rvert^\delta sgn(\varphi)$	$t = 0, h \to 0$	$\delta = 3$
Correlation length	ν	$\xi \propto \lvert t\rvert^{-\nu}$	$t \to 0, h = 0$	$\nu = \frac{1}{2}$
Correlation function	η	$G(r) \propto \lvert r\rvert^{-d+2-\eta}$	$t = 0,\ h = 0$	$\eta = 0$
dynamic	z	$\tau_c \propto \xi^z \propto \lvert t\rvert^{-\nu z}$	$t \to 0, h = 0$	N/A

We have also quoted the dynamical exponent z which describes the relation between the diverging correlation time, τ_c, and the diverging correlation length, ξ, according to $\tau_c \propto \xi^z$. As we will discuss in Chapter 5, this exponent plays a special role in classical critical phenomena, as statics and dynamics decouple in a well-defined sense.

Critical phenomena display a high degree of *universality*. This means that critical exponents are identical for classes of phase transitions, the so-called universality classes: The exponents depend only on the dimensionality of the system and the symmetry of

the order parameter.[1] Consequently, e.g. all systems with Ising order parameter in three dimensions share the same critical exponents.

Universality is rooted in the divergence of the correlation length: Given that critical phenomena are determined by the physics at large length scales, microscopic details become unimportant.

2.4 Scaling hypothesis

The scaling hypothesis is based on the assumption that, near a critical point, the order-parameter correlation length ξ is the only relevant length scale.[2] The concept of scaling is exposed by considering the behavior of the system under the *scaling transformations*.

$$\begin{aligned} x &\to bx && \text{lengths} \\ t &\to b^{y_t} t && \text{reduced temperature} \\ h &\to b^{y_h} h && \text{external field} \end{aligned} \tag{2.20}$$

Here, the changes of the parameters t, h compensate for the change in length scale: The physics should be invariant under such a transformation (for appropriate y_t, y_h), because the change of ξ upon a change of parameters t, h corresponds to a change of the reference length scale.

Scaling hypothesis for the free energy density (more precisely for the singular part of it, f_s) is

$$f_s(t, h) = b^{-d} f_s(b^{y_t} t, b^{y_h} h) \tag{2.21}$$

for any value of b, which is the mathematical statement of a generalized homogeneity law.

To gain insight, we first consider $h = 0$. The transformation $|t| \to b^{y_t}|t|$ causes the correlation length to change as $\xi \to b^{-\nu y_t}\xi$ (because $\xi \sim |t|^{-\nu}$). Requiring invariance of physics under the combined transformation (2.20), this change must be undone by the changes of length scales $x \to bx$, which implies $\nu y_t = 1$ or $y_t = \frac{1}{\nu}$. Thus, use $b = |t|^{-1/y_t} = |t|^{-\nu}$ and get the power law behaviour of the free energy density

$$f_s(t, h = 0) = |t|^{d\nu} f_s(1, 0) \tag{2.22}$$

where $f_s(1, 0) = \text{const}$.

From f_s one can derive all critical exponents and relate them to y_t, y_h. There exist only *two* independent critical exponents for static critical phenomena. Therefore there

[1] In addition to dimensionality and order-parameter symmetry, the character of the interactions can also be relevant for determining the universality class of a system: systems with long-ranged interactions behave differently as compared to those with short-ranged interactions.

[2] See Goldenfeld's book [2] for an exposition on why microscopic length scales are required for the existence of anomalous exponents.

exist several scaling relations, like e.g.

$$\begin{aligned} 2-\alpha &= d\nu\,, \\ 2-\alpha &= 2\beta+\gamma\,, \\ 2-\alpha &= \beta(\delta+1)\,. \end{aligned}$$

Other forms of the scaling hypothesis: Eliminate y_t by fixing $b = |t|^{-\nu}$ and get, e.g.

$$f_s(t,h) = |t|^{d\nu} f_s(1, \frac{h}{|t|^{\nu y_h}}) \tag{2.23}$$

The scaling hypothesis for the correlation function, e.g. reads:

$$G(r;t,h) = \frac{1}{r^{d-2+\eta}} f_G\left(\frac{r}{\xi}; \frac{h}{|t|^{\nu y_h}}\right) \tag{2.24}$$

where at the critical point $\xi \to \infty, h \to 0$ and $G(r) = \frac{1}{r^{d-2+\eta}} f_G(0,0)$. Now we can relate η to other critical exponents by looking at the definitions of the exponents

$$\begin{aligned} \chi \sim \int d^d r G(r) &\propto \int dr\, f_G\left(rt^{\nu}, \frac{h}{t^{\nu y_h}}\right) r^{1-\eta} \\ &= \int dx\, f_G\left(x, \frac{h}{t^{\nu y_h}}\right) x^{1-\eta} \frac{1}{t^{(2-\eta)\nu}} \\ &\sim t^{-\gamma} \quad (\text{at } h=0) \end{aligned}$$

using the substitution $x = r|t|^{\nu}$, and after doing the last integral, one gets a relation $\gamma = \nu(2-\eta)$.

At the level of the present discussion, the scaling hypothesis is a hypothesis. It can be justified using RG tools. As we will see later, this simple form of the scaling hypothesis (often dubbed "naive scaling") only holds below the upper critical dimension, $d < d_c^+$ (recall $d_c^+ = 4$ for magnets). For $d > d_c^+$ naive scaling is violated due to the presence of dangerously irrelevant variables. In this case, some of the scaling laws do not hold – this applies to so-called hyperscaling laws which involve the spatial dimension d (and scaling laws derived from them).

Chapter 3

Renormalization group

3.1 Concept of RG

In a typical condensed-matter setting, we are often interested in the physics at large length or time scales and at low energies, because the long-distance behavior of correlation functions contains the information about spontaneous symmetry breaking and hence about the phase. This is obvious for a magnet: a short-distance correlator, e.g., between neighboring spins, is finite at any temperature, whereas the correlation function in the long-distance limit is zero above T_C and finite below T_C.

To access the long-distance, low-energy behavior efficiently, renormalization-group approaches successively eliminate short-distance/high-energy degrees of freedom such that the long-distance behavior remains unchanged. Generically, a decimation step modifies both the model itself and its coupling constants. Often, however, one can combine the decimation step with a scaling transformation such that the model remains invariant, and only its coupling constants change. This "renormalization-group flow" of coupling constants under successive decimation of high-energy degrees of freedom (leading to "running coupling constants") is a central object in RG calculations.

Following the RG flow to longer and longer length scales (or smaller and smaller energies), the coupling constants will usually flow to asymptotic values (so-called fixed point values). Fixed point values are either trivial – 0 or ∞, corresponding to stable phases – or they are non-trivial, i.e., finite, corresponding to continuous phase transitions.[1]

Example: For a lattice spin model of a ferromagnet one can think of a simple real-space decimation scheme, dubbed block-spin RG, see figure 3.1: Here, in each step the lattice is divided into supercells, and the spins in each cell are joined into a superspin. This maps the coupling constant J onto a new coupling constant J'.

Successive decimation steps define a discrete RG flow of J. The fixed points of this flow are easily interpreted: $J \to 0$ implies decoupled spins and hence corresponds to the

[1]First-order phase transitions do not have a straightforward signature in RG. Often, the RG is characterized by run-away flow, but other situations are possible. We will not discuss this further.

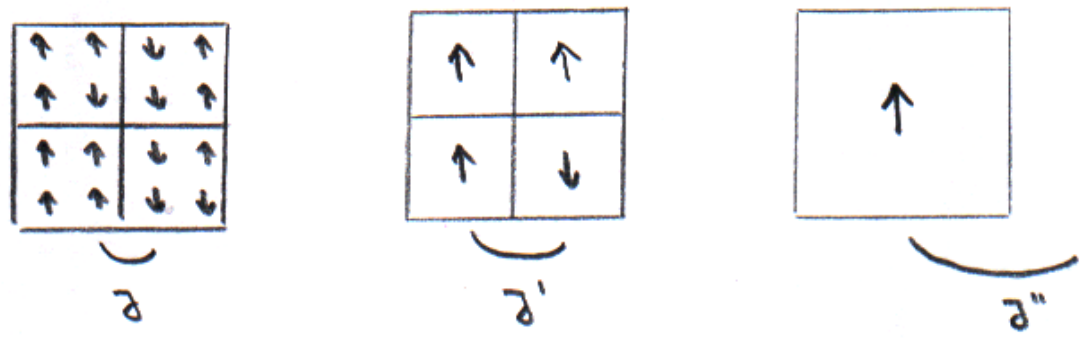

Figure 3.1: Schematic representation of block-spin RG.

disordered (i.e. high-temperature) phase. In contrast, $J \to \infty$ implies spins being locked together and corresponds to the symmetry-broken ordered (i.e. low-temperature) phase. A typical flow diagram is shown for the block-spin RG in figure 3.2.

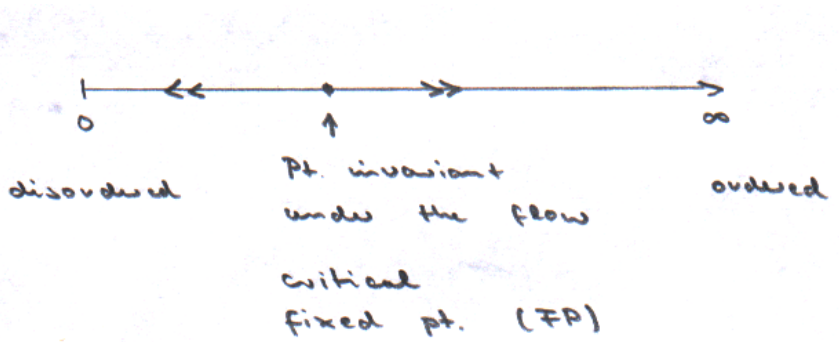

Figure 3.2: Generic RG flow diagram for a lattice spin system, as can be obtained from block-spin RG.

3.2 Scaling transformation and scaling dimension

Each RG step involves – in addition to the decimation of degrees of freedom – a rescaling of lengths and momenta to account for the change of the "observation scale". Explicitly, lengths and momenta change according to

$$k' = sk \,, x' = x/s \tag{3.1}$$

where $s > 1$ is a rescaling factor. In many cases, RG transformations are performed in infinitesimal steps, such that a parametrization $s = e^{dl}$ with infinitesimal dl is useful. Then, the RG flow is described by differential equations.

Model parameters (fields, coupling constants) will change under scaling transformations as well; usually their transformation behavior is fixed within a certain RG scheme by imposing suitable invariance conditions onto the model, see below for examples.[2]

For infinitesimal transformations, it is useful to introduce the concept of a **scaling dimension** of a model parameter Q: Under scaling transformation $x' = x/s$ it changes as

$$Q' = Q s^{\dim[Q]} \tag{3.2}$$

which defines $\dim[Q]$. The concept of scaling dimensions is particularly useful to classify small perturbations to a particular RG fixed point: The sign of $\dim[Q]$ decides whether Q grows or shrinks along the RG flow. Accordingly, one distinguishes the cases

$\dim[Q] > 0$	relevant parameter
$\dim[Q] < 0$	irrelevant parameter
$\dim[Q] = 0$	marginal parameter

In a differential RG equation, the scaling dimension appears as prefactor of the linear term:

$$\frac{dQ}{dl} = \dim[Q] Q + \dots \tag{3.3}$$

with the dots representing higher-order terms: The left-hand side is a Taylor expansion in powers of Q, with the constant term being absent as $Q = 0$ is assumed to be a fixed point. For $\dim[Q] = 0$ the higher-order terms determine the fate of Q under RG flow, and one distinguishes marginally relevant, marginally irrelevant, or exactly marginal perturbations (in the latter case, Q does not flow to all orders).

As a relevant perturbation to a fixed point grows under RG, it implies that the state represented by the fixed point is not stable at low energies. Conversely, if a particular fixed point represents a stable phase, then all symmetry-preserving perturbations should be irrelevant. For example, chemical-potential disorder is a relevant perturbation to a Fermi gas in one or two space dimensions, leading to Anderson localization, whereas it is an irrelevant perturbation in $d = 3$.

3.3 Momentum-shell RG for the $\mathbb{O}(N)$ ϕ^4 model

We now demonstrate the working principles of RG using a concrete example. Consider a classical N-component ϕ^4 model in d space dimensions, described by the effective

[2] In principle, the choice of an RG scheme for a given model is not unique. Different RG schemes may lead to different intermediate-step results, but their answers for physical observables agree. In many cases, a direct interpretation of the RG flow is useful and justified, but needs to be done with care as the running couplings are in general not observable.

Hamiltonian

$$H = \int d^d x \left(\frac{1}{2} (\partial_x \varphi)^2 + \frac{1}{2} r \varphi^2(x) + \frac{u}{4!} \varphi^4(x) \right) \tag{3.4}$$

$$= \int_0^\Lambda \frac{d^d k}{(2\pi)^d} \frac{1}{2} \left(k^2 \varphi(k)^2 + r \varphi^2 \right) + \frac{u}{4!} \int \frac{d^d k_1 d^d k_2 d^d k_3}{(2\pi)^{3d}} \varphi(k_1)\varphi(k_2)\varphi(k_3)\varphi(-k_1-k_2-k_3) \tag{3.5}$$

where r is the tuning parameter of the phase transition (often dubbed "mass"), u the order-parameter self-interaction, and Λ the physical ultraviolet momentum-space cutoff related to the lattice constant a as $\Lambda \sim \frac{\pi}{a}$. The form of this theory is identical to that of Ginzburg-Landau theory (2.10), and the fields have been scaled such that the prefactor of the gradient term is unity. As we will see below, it pays to consider the ϕ^4 model (3.4) for arbitrary values of the space dimension d, including non-integer ones. The critical exponents will then be continuous functions of d, and the perturbative calculation described below will evaluate exponents in $d = 4 - \epsilon$ dimensions.

In particular in view of quantum generalizations to be described later, it is useful to re-interpret H (3.4) – up to a factor $\beta = 1/(k_B T)$ – as an action S which is related to the partition function Z by $Z = \int \mathfrak{D}[\phi(r)] \exp(-S)$.[3]

The recipe for the so-called momentum-shell RG is to eliminate degree of freedom in momentum space in a differential fashion. It can be summarized as follows.

1. Separate degrees of freedom

$$\varphi(k) = \begin{cases} \varphi_< & k < \dfrac{\Lambda}{s} \quad \text{with } (s > 1) \\ \varphi^> & \dfrac{\Lambda}{s} < k < \Lambda \end{cases} . \tag{3.6}$$

2. Integrate out $\varphi_>$ (while preserving Z), i.e. renormalize the couplings r, u.

3. Rescale momenta, lengths, fields, couplings, etc. to restore the action with cutoff Λ.

RG for Gaussian model: We first demonstrate these steps for the Gaussian model, with quartic coupling $u = 0$. We combine the rescaling (3.1) with a rescaling of the fields to

$$\begin{aligned} k' &= sk \,, \\ x' &= x/s \,, \\ \varphi'(k') &= \varphi_<(k) s^a \,. \end{aligned}$$

The RG steps are:

[3]We note that the kinetic-energy piece is missing from H, as thermodynamic properties of classical critical phenomena are determined by the potential energy only. Hence, there is no distinction between Lagrangian and Hamiltonian at this point.

1. Separate degrees of freedom:

$$Z = \int \mathfrak{D}[\varphi_<] \int \mathfrak{D}[\varphi_>] \exp\left(- \int^{\Lambda/s} d^d k (k^2 + r)\varphi_<^2 - \int_{\Lambda/s}^{\Lambda} d^d k (k^2 + r)\varphi_>^2 \right) \quad (3.7)$$

   where prefactors of 2 and π have been omitted.

2. Integrate over fields with large momenta. The resulting renormalization is trivial: For non-interacting fields, eliminating $\varphi_>$ does not change the action for $\varphi_<$.

3. Rescale momenta, lengths, fields, couplings, etc. to restore the action – this fixes the parameter a of the scaling transformation and results in a transformation rule for r.

$$\begin{aligned} S_< &= \int^{\Lambda/s} d^d k \varphi_<(k)^2 (k^2 + r) = \int^{\Lambda} \frac{d^d k'}{s^d} \varphi'(k')^2 s^{-2a} \left((k'/s)^2 + r \right) \\ &= \int^{\Lambda} d^d k' \varphi'(k')^2 (k'^2 + r') \end{aligned}$$

   where $a = -\frac{d+2}{2}$ and therefore $r' = s^2 r$.[4]

Now we consider a differential RG step using $s = e^{dl}$, hence $dr = 2dlr$, and obtain the RG equation for the coupling r:

$$\frac{dr}{dl} = 2r \,. \quad (3.8)$$

Fig. 3.3 shows two stable fixed points at $r = +\infty$ and $r = -\infty$ which correspond to the disordered and ordered phases of Ginzburg-Landau theory, respectively. At $r = 0$ there is an unstable fixed point, where the model is scale-invariant. This fixed point, dubbed Gaussian fixed point, is a critical fixed point controlling the phase transition.

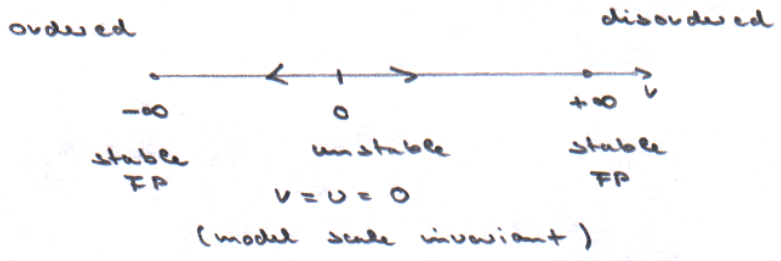

Figure 3.3: RG flow for the Gaussian model derived from Eq. (3.8), showing two stable fixed points at $r = \pm\infty$ and one unstable fixed point at $r = 0$.

[4]Our rescaling fixes the prefactor of the gradient term to unity; other rescaling schemes are possible as well and lead to the same physical results.

RG for ϕ^4 model: We now include the quartic coupling u of the φ^4 model, treating u perturbatively. As we will see below, this is justified close to and above four space dimensions. We start with the contributions to first order in u:

$$\begin{aligned} Z &= \int \mathfrak{D}[\varphi_>]\mathfrak{D}[\varphi_<] \exp\left(-S_0^< - S_0^> - \text{“}u\varphi^4\text{”}\right) \\ &= \int \mathfrak{D}[\varphi_<] \exp\left(-S_0^<\right) \int \mathfrak{D}[\varphi_>] \exp\left(-S_0^>\right) \times (1 - \text{“}u\varphi^4\text{”}) \end{aligned}$$

where “$u\varphi^4$” is a term linear in u given by $\varphi^>\varphi^>\varphi^<\varphi^<$. Upon performing the integral over $\varphi_>$, the contribution from the u term can be represented in the form of Feynman diagrams, shown in figure 3.4. Keeping only the zero-momentum piece of the external

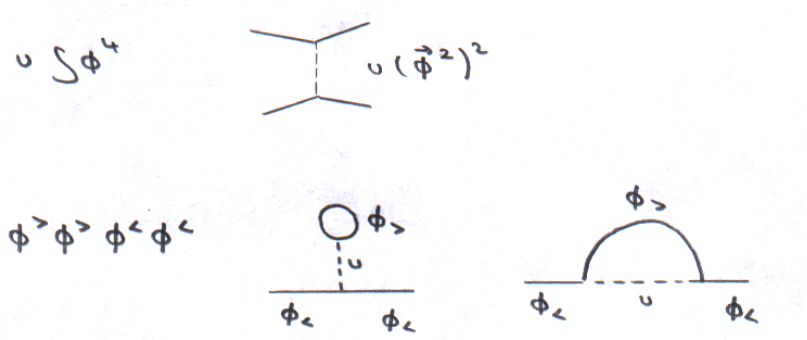

Figure 3.4: Top: Graphical representation of the quartic interaction. Bottom: Feynman diagrams to linear order in u – both induce a renormalization of the coupling constant r.

fields $\varphi_<$, both diagrams contribute to the renormalization of r. Together with the rescaling step, we arrive at

$$r' = s^2 \left(r + u \frac{N+2}{6} \int_{\Lambda/s}^{\Lambda} \frac{d^d k}{(2\pi)^d} \frac{1}{k^2 + r} \right) . \tag{3.9}$$

At this point, a few remarks on the construction of Feynman diagrams for the perturbative corrections to the action are in order. (i) All internal lines must represent $\varphi^>$ propagators, because these are the fields which are integrated over, whereas all external lines must corresponds to $\varphi^<$. (ii) All contributions with odd powers of $\varphi^>$ drop out, as they yield Gaussian integrals over odd functions.

It turns out that a consistent determination of a non-trivial RG flow requires to go to second order in u. The resulting diagrams are shown in Figs. 3.5, 3.6, and 3.7. The diagram in Fig. 3.5 is of two-loop order; as we will see below, this contributes only to second order in an expansion in $\epsilon = 4 - d$ and will be neglected here. The diagram in Fig. 3.6 generates a φ^6-term which can be shown to be strongly irrelevant near $d = 4$; it

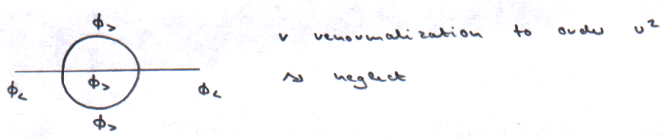

Figure 3.5: Second-order Feynman diagram leading to a renormalization of r to order u^2 (neglect this).

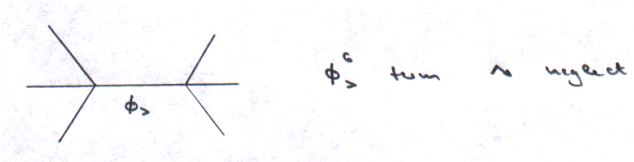

Figure 3.6: Second-order Feynman diagram inducing a φ^6 term (neglect this).

can also be neglected. Finally, the diagram in figure 3.7 induces a renormalization of u, being important for the RG flow. Together with the rescaling step, the transformation for u reads

$$u' = s^{4-d}\left(u - u^2\frac{N+8}{6}\int_{\Lambda/s}^{\Lambda}\frac{d^dk}{(2\pi)^d}\frac{1}{(k^2+r)^2}\right). \tag{3.10}$$

It is useful to trade r and u for dimensionless variables t and g, defined by:

$$r = t\Lambda^2$$
$$u = g\frac{\Lambda^{4-d}(2\pi)^d}{S_d}$$

where S_d is the surface of a d-dimensional sphere.

RG equations: Evaluating the diagrams then yields the RG equations for the variables t and g:

$$\frac{dt}{dl} = 2t + \frac{N+2}{6}\frac{g}{1+t} + \mathcal{O}(g^2), \tag{3.11}$$
$$\frac{dg}{dl} = (4-d)g - \frac{N+8}{6}\frac{g^2}{(1+t)^2} + \mathcal{O}(g^3). \tag{3.12}$$

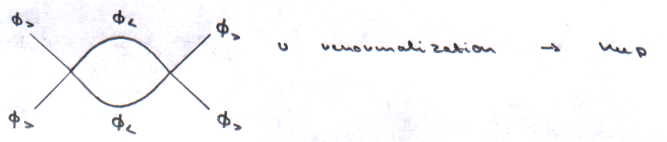

Figure 3.7: Second-order Feynman diagram leading to a renormalization of u (keep this).

where the last terms represent the influence of higher-order diagrams – recall that these RG equations are based on an expansion in the quartic coupling and as such require g to be small.

3.3.1 Fixed points

We now discuss the fixed points of the RG equations (3.11), concentrating on the vicinity of the phase transition for small $|t|$. (As before, $t \to \pm\infty$ correspond to the disordered and ordered phases, respectively.) First, we observe that the Gaussian fixed point

$$t^\star = g^\star = 0 \tag{3.13}$$

remains a fixed point of the RG flow. It is useful to state the scaling dimensions of the couplings with respect to this fixed point which can be read off from the linear term of the corresponding RG equation:

$$\dim[r] \equiv \dim[t] = 2\,, \tag{3.14}$$
$$\dim[u] \equiv \dim[g] = 4 - d\,, \tag{3.15}$$

i.e., the quartic coupling is irrelevant for $d > 4$, as will be discussed in more detail below. We also note that higher-order terms are typically more irrelevant, e.g., the coefficient of a ϕ^6 term is characterized by

$$\dim[u_6] = 6 - 2d \tag{3.16}$$

and hence irrelevant for $d > 3$.

In addition to the Gaussian fixed point there is another fixed point at finite t and g, with $g^\star \sim (4-d)(1+t)^2$. Requiring that g should be small – only then the perturbative treatment is valid – implies that $(4-d)$ needs to be small (assuming $|t| \ll 1$). Introducing

$$\epsilon = 4 - d \tag{3.17}$$

we find the second fixed point as

$$g^\star = \frac{6}{N+8}\epsilon + \mathcal{O}(\epsilon^2)\,, \tag{3.18}$$
$$t^\star = -\frac{1}{2}\frac{N+2}{N+8}\epsilon + \mathcal{O}(\epsilon^2)\,. \tag{3.19}$$

This is the so-called Wilson-Fisher fixed point. Note that the $(1 + t)$ terms in the denominators in Eq. (3.11) have been approximated by unity, as they contribute to higher orders in ϵ only. It turns out that the expansion terms for the fixed-point values (and for physical observables) can be systematically organized in a loop expansion: Contributions at order ϵ^n arise from Feynman diagrams with n closed loops.

For $d > 4$ the Gaussian fixed point controls the transition, as seen in figure 3.8, while the Wilson-Fisher fixed point controls the transition for $d < 4$ (figure 3.9). The flow

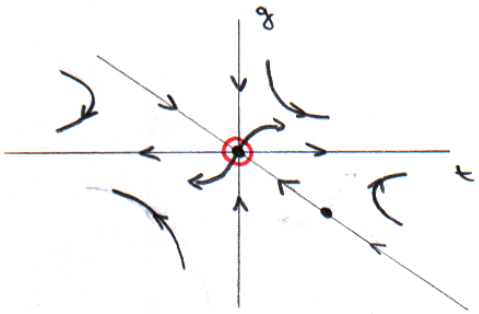

Figure 3.8: RG flow of the ϕ^4 model for $d > 4$.

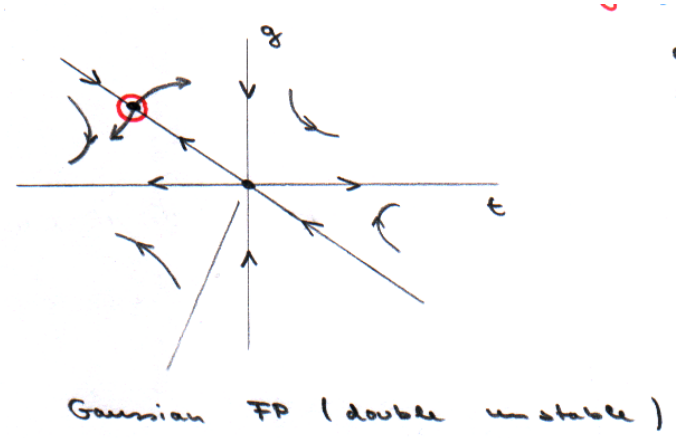

Figure 3.9: RG flow of the ϕ^4 model for $d < 4$.

diagrams feature a separatrix which separates the flow to the disordered fixed point from the one to the ordered fixed point; the critical fixed point is located on this separatrix.[5]

It is useful to make contact between the RG flow diagram and experimental systems. In an experiment, one typically varies a single parameter (most often temperature) to access a phase transition. Each set of experimental parameters corresponds to one initial set of couplings of the ϕ^4 model; hence, the experimental conditions define a line (parameterized by temperature) in the RG flow space. This line usually does not hit the critical fixed point, but crosses the separatrix as illustrated in figure 3.10. This crossing corresponds to the physical phase transition point, $T = T_c$, where the RG flow is towards the critical fixed point. At any other temperature, the flow is either towards $t \to +\infty$, i.e., the disordered phase, or $t \to -\infty$, i.e., the ordered phase.

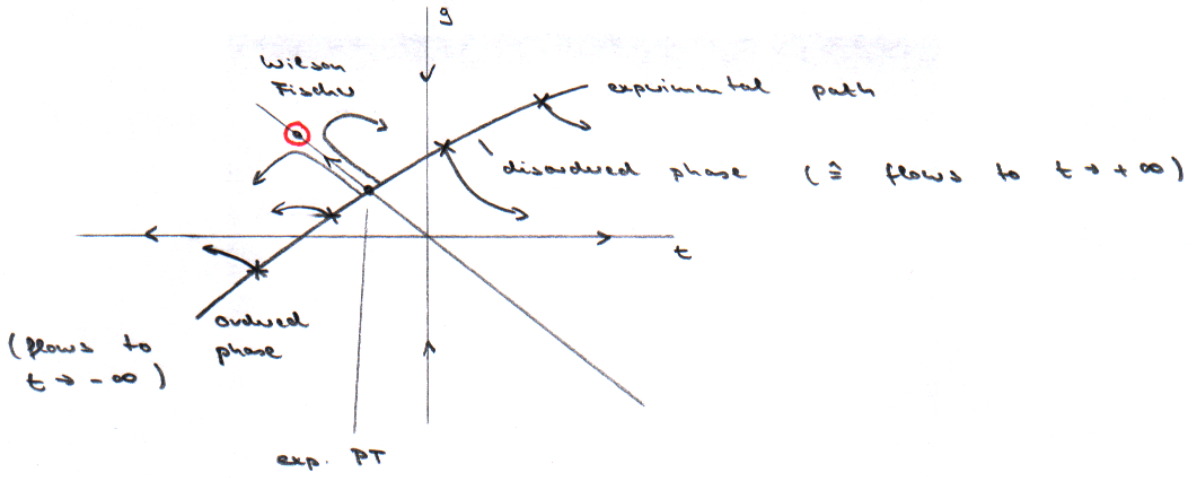

Figure 3.10: RG flow diagram with trajectory of typical experimental initial conditions together with the resulting RG flow.

Perturbations to the Wilson-Fisher fixed point: It is useful to analyze the flow in the vicinity of the critical fixed point in more detail. To this end, we re-write the RG equations using the parametrization

$$t = t^\star + \delta t\,, \tag{3.20}$$
$$r = r^\star + \delta r\,, \tag{3.21}$$

[5] In a n-dimensional space of coupling constants, the separatrix is a $(n-1)$ dimensional surface.

with the fixed-point values $g^\star = \frac{6}{N+8}\epsilon + O(\epsilon^2)$ and $t^\star = -\frac{N+2}{2(N+8)}\epsilon + O(\epsilon^2)$. Keeping only first-order terms in the deviations δt, δr we arrive at the linearized RG equations

$$\frac{d\delta t}{dl} = \delta t \left(2 - \epsilon \frac{N+2}{N+8}\right) + \delta g \frac{N+2}{6}\left(1 + \epsilon \frac{N+2}{N+8}\right) \tag{3.22}$$

$$\frac{d\delta g}{dl} = -\epsilon \delta g \,. \tag{3.23}$$

These equations can be solved by writing them in a matrix form: diagonalizing the matrix yields eigenvalues, representing the scaling dimensions of the perturbations about the fixed point, and the corresponding eigenvectors, reflecting the flow directions. For the Wilson-Fisher fixed point in spatial dimensions $d < 4$ there is one irrelevant direction and one relevant direction.

In general, the scaling dimension of most relevant perturbation X to a critical fixed point is identical to the inverse correlation length exponent,

$$\dim[X] = \frac{1}{\nu}, \tag{3.24}$$

because a *generic* deviation from the critical fixed point has a component along X, hence X represents a tuning parameter of the phase transition with $\xi \sim X^{-\nu}$. The behavior under scaling transformations $X' = X s^{\dim[X]}$ and $\xi' = \xi/s$ (as $\dim[\xi] = -1$) then dictates Eq. (3.24). This reasoning also implies that $\frac{1}{\nu}$ is a measure of how fast (in terms of RG flow) a system is driven away from criticality.

For the Wilson-Fisher fixed point we have $X \equiv \delta t$ and hence

$$\nu = \frac{1}{2} + \frac{\epsilon(N+2)}{4(N+8)} \tag{3.25}$$

whereas the Gaussian fixed point simply has $\nu = \frac{1}{2}$ as in Ginzburg-Landau theory.

A few further remarks:

- A critical fixed point has a single relevant perturbation, i.e., one flow eigenvector with positive scaling dimension.

- Fixed points with more than one relevant perturbation correspond to multi-critical points: To reach such a point experimentally requires fine tuning of more than one parameter.

- The RG demonstrated here for the classical d-dimensional ϕ^4 model applies unchanged to the quantum φ^4 model (see Section 5.3) at $T = 0$ in $(d-1)$ space dimensions.

3.3.2 Field renormalization and anomalous exponent

We now supplement the RG analysis with a determination of the anomalous exponent η of the order-parameter correlations. This analysis also illustrates how to actually calculate observables at criticality in renormalized perturbation theory: One performs bare low-order perturbation theory in u, then replaces u by its fixed-point value, and expands the result for small ϵ to yield the desired form (e.g. a power law). This strategy of a double expansion (in both u and ϵ) is key in applications of perturbative RG.

The exponent η is defined by the behavior of the correlator at criticality:

$$\langle\phi(k)\phi(-k)\rangle \sim \frac{1}{k^{2-\eta}}\,. \tag{3.26}$$

Treating the ϕ^4 perturbatively yields the form

$$\langle\phi(k)\phi(-k)\rangle = \frac{1}{k^2 + r - \Sigma(k)} \tag{3.27}$$

where r is the bare mass, and $\Sigma(k)$ contains all contributions arising from the quartic coupling u. The critical point is defined by $r = \Sigma(k = 0)$, i.e., a vanishing renormalized mass. Hence, a non-trivial momentum dependence at criticality arises from $\Sigma(k)-\Sigma(k = 0)$. The lowest-order contribution to this arises from the diagram in Fig. 3.5 which, evaluated for $d = 4$, yields

$$\Sigma(k) - \Sigma(k = 0) = c_1 u^2 k^2 \ln \Lambda/k \tag{3.28}$$

with c_1 a constant. Expressing this using the coupling t and inserting its fixed-point value gives

$$\langle\phi(k)\phi(-k)\rangle = \frac{1}{k^2 - c_2 g^{\star 2} k^2 \ln \Lambda/k}\,. \tag{3.29}$$

This is not yet the desired power law, the reason being that higher-order contributions will produce additional log-divergent terms, and only the combination of all of them yields a power law. A small-ϵ approximation to the anomalous exponent can be obtained using the relation $k^x \approx 1 + x \ln k$, valid for small x:

$$\langle\phi(k)\phi(-k)\rangle = \frac{1}{k^2}\frac{1}{1 - c_2 g^{\star 2} \ln \Lambda/k} \approx \frac{1}{k^2}\left(\frac{\Lambda}{k}\right)^{c_2 g^{\star 2}}\,. \tag{3.30}$$

The last step, which is an expansion for small $g^\star$, effectively re-sums a series of higher-order contributions. Comparing to Eq. (3.26) we read off $\eta = -c_2 g^{\star 2}$. Re-instating the constants we finally have

$$\eta = \frac{N + 2}{2(N + 8)^2}\epsilon^2. \tag{3.31}$$

The first contribution to η being of two-loop order implies, combined with the small prefactor, that η is numerically small for phase transitions in the ϕ^4 model.

3.4 Phase transitions and critical dimensions

We now turn to a more general discussion of the order–disorder phase transition of ϕ^4 models in arbitrary dimension d and for arbitrary number of order-parameter components N. First, we establish the notion of upper and lower critical dimension.

Critical dimensions:

- The upper critical dimension d_c^+ is defined by the fact that for $d \geq d_c^+$ mean-field theory is asymptotically exact.
- The lower critical dimension d_c^- is defined by the fact that for $d \leq d_c^-$ fluctuations destroy the ordered phase at any temperature.
- Critical exponents typically take non-trivial d-dependent values for $d_c^- < d < d_c^+$ whereas they take d-independent mean-field values for $d > d_c^+$.[6]
- Classical magnets (described by ϕ^4 models) with short-range interactions have $d_c^+ = 4$ and $d_c^- = 2$ for $N > 2$ or $d_c^- = 1$ for $N = 1$ (see below for $d = 2$, $N = 2$).

Let us discuss the physics of the upper critical dimension in more detail, based on the RG flow for the ϕ^4 model derived above.

- For $d < d_c^+ = 4$, the quartic coupling u is relevant, such that the phase transition is controlled by the Wilson-Fisher fixed point. In calculations of observables, the coupling u can be replaced by its fixed-point value $u^\star$ and the cutoff Λ can be sent to ∞. As a result, suitably defined observables (like dimensionless crossover functions) will be fully universal, i.e., independent of the initial values of u and Λ. Exponents will depend on the fixed-point value of u and hence vary with d. Naive scaling is typically valid, and the critical exponents fulfill hyperscaling relations.
- For $d > 4$, u is irrelevant and the exponents will take mean-field values. Further, integrals for observables are typically ultra-violet divergent, such that the cutoff Λ has to be kept finite and crossover functions acquire non-universal contributions. Naive scaling does necessarily not apply, and hyperscaling relations are violated.
- For $d = 4$, u is marginally irrelevant, resulting in logarithmic corrections to mean-field behavior.
- Attention: The quartic coupling u is *dangerously* irrelevant for $d \geq 4$. Although $u^\star = 0$ at the Gaussian fixed point, a finite u is required in the calculation of certain observables (like the magnetization in the ordered phase). Near-critical observables will then depend on the initial value of u, although the fixed-point value is zero.

[6] For models with long-range interactions, mean-field exponents may depend on d.

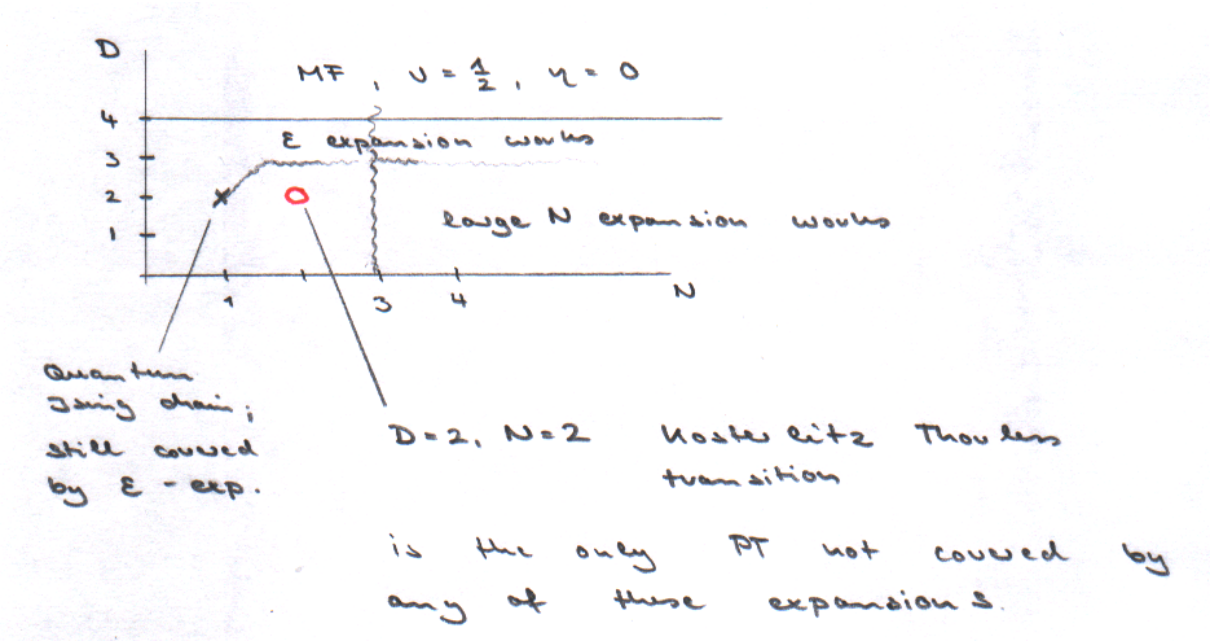

Figure 3.11: Overview of transitions of the $\mathbb{O}(N)$ model in a plane spanned by the number of spatial dimensions d and the number of order-parameter components N, showing the applicability ranges of mean-field theory, $(4-\epsilon)$ expansion, and $1/N$ expansion.

The momentum-shell RG for the ϕ^4 model, combined with the expansion in the quartic coupling u, is controlled by the small parameter $\epsilon = 4 - d$. Hence, it gives reliable results close to and above the upper-critical dimension. Further, it turns out that it gives qualitatively correct results even for $\epsilon = 1$, i.e., for $d = 3$.[7]

There are various alternative ways to analytically calculate critical exponents, which employ different limits. One option is a $1/N$-expansion where N is the number of order-parameter components: It turns out that the case $N = \infty$ can be solved exactly using a certain mean-field theory, and a controlled expansion in $1/N$ is feasible. Another option is an expansion about the lower critical dimension: For $d = d_c^- + \epsilon$ the ordering temperature $T_c \sim \mathcal{O}(\epsilon)$, such that T_c itself becomes a small parameter of the theory. For magnets, this "$2+\epsilon$" expansion, which is performed as an expansion around the ordered phase, can be used to access critical exponents as well.

A summary of the utility of expansions for magnetic system is given in figure 3.11. A special case is $d = 2$, $N = 2$ which is not correctly described by any of the expansions: While long-range order is absent at any finite T, there exists quasi-long-range order with power-law correlations below a transition temperature T_c. The transition between this low-temperature and the disordered high-temperature phase is a Kosterlitz-Thouless transition driven by the unbinding of vortex–antivortex pairs, i.e., topological defects.

[7] Higher-order ϵ expansions, together with suitable extrapolation schemes, can often be used to obtain accurate quantitative estimates of exponents for $\epsilon = 1$.

Chapter 4

Theoretical models for quantum phase transitions

With this chapter, we turn to phase transitions taking place at zero temperature, so-called quantum phase transitions (QPT). We start by introducing a few basic lattice models which such QPT. In general, the models are characterized by the competition between two Hamiltonian terms, one favoring long-range order and one promoting local quantum fluctuations which tend to destroy order.

4.1 Quantum Ising model

A quantum Ising model – often also called transverse-field Ising model – consists of localized spin-1/2 objects placed on a regular lattice, with the Hamiltonian

$$H_I = -J \sum_{\langle ij \rangle} \sigma_i^z \sigma_j^z - Jg \sum_i \sigma_i^x \tag{4.1}$$

where σ^α with $\alpha = x, y, z$ are Pauli matrices representing spins 1/2. The first term is the conventional Ising interaction, and the second encodes an external magnetic field in a direction perpendicular to the Ising axis, such that the model features a $\mathbb{Z}_2$ symmetry corresponding to $\sigma_i^z \leftrightarrow -\sigma_i^z$. Here J represent the overall energy scale, and the dimensionless parameter g controls the behavior of the system at $T = 0$.

The limiting cases are easily discussed:

Limit $g \to 0$: The ground state will be the perfectly aligned state $|\uparrow\rangle = \prod_i |\uparrow\rangle_i$ or $|\downarrow\rangle = \prod_i |\downarrow\rangle_i$.This state has a spontaneously broken Z_2 symmetry. For small finite g, flipped spins will admix into the ground state, but the Z_2 symmetry remains broken.

This ordered state is characterized by the order parameter $\langle 0| \sigma_i^z |0\rangle = \pm N_0$, representing a uniform magnetization (per site), i.e., a ferromagnet.

Limit $g \to \infty$: The ground state is $|0\rangle = \prod_i |\rightarrow\rangle_i$, i.e., the spins are polarized in field direction. For large finite g, pairs of antialigned spins admix into the ground state.

This disordered state does not break any symmetries of the Hamiltonian.

Hence, a $T = 0$ phase transition must occur upon variation of g: lowering g from large values leads to the onset of order at $g = g_c$, see Fig. 4.1. As we will discuss later, this quantum phase transition in d space dimensions is in the universality class of the $d + 1$-dimensional classical Ising model.

For space dimensions $d \geq 2$ the Ising order also exists at finite temperature, resulting in a phase diagram as shown in Fig. 4.2.

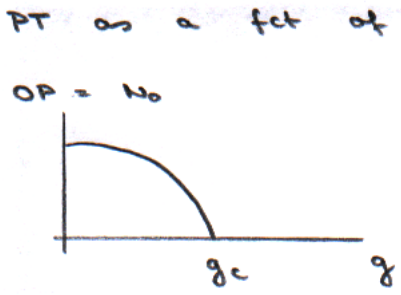

Figure 4.1: Order parameter of the quantum Ising model as function of the tuning parameter g.

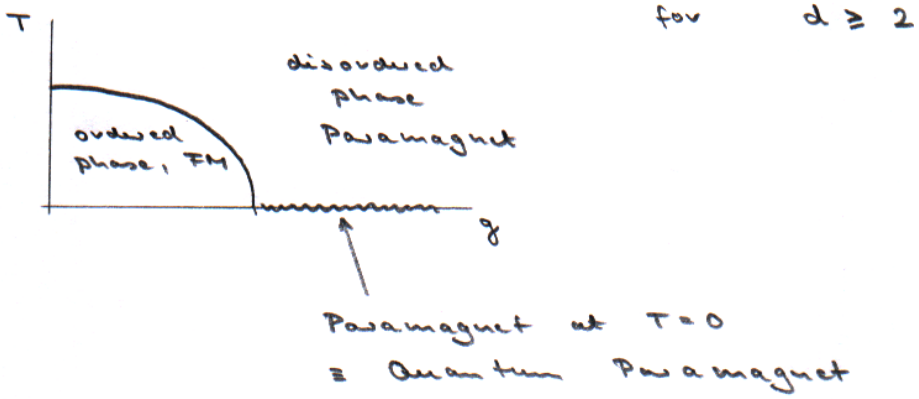

Figure 4.2: Finite-temperature phase diagram of the quantum Ising model.

The quantum Ising model, with an experimentally accessible quantum phase transition, can be realized in magnetic insulators with ferromagnetic interactions and a strong Ising anisotropy. Two examples are $LiHoF_4$ [5], a three-dimensional Ising system (which, however, has long-range dipolar instead of nearest-neighbor interactions) and $CoNb_2O_6$ [6], a quasi-one-dimensional system.

4.2 Quantum rotor model

A quantum rotor can be visualized as a particle moving on a N-dimensional unit sphere ($N \geq 2$), with orientation $\vec{n}$ and the constraint $\vec{n}^2 = 1$. The quantum dynamics of a rotor is captured by a conjugate momentum $\vec{p}$, defined by

$$[n_\alpha, p_\beta] = i\delta_{\alpha\beta} \tag{4.2}$$

in units where $\hbar = 1$. It is convenient to define the rotor angular momentum by

$$L_{\alpha\beta} = n_\alpha p_\beta - n_\beta p_\alpha \tag{4.3}$$

which has $N(N-1)/2$ components. For the important case $N = 3$ we may introduce the familiar vectorial notation $L_\alpha = (1/2)\epsilon_{\alpha\beta\gamma}L_{\beta\gamma}$ with $\epsilon_{\alpha\beta\gamma}$ the antisymmetric tensor. Then the commutation relations read:

$$[L_\alpha, L_\beta] = i\epsilon_{\alpha\beta\gamma}L_\gamma$$
$$[L_\alpha, n_\beta] = i\epsilon_{\alpha\beta\gamma}n_\gamma$$

For any $N \geq 2$ the kinetic part of the Hamiltonian of a single rotor is

$$H_K = \frac{Jg}{2}\vec{L}^2 \tag{4.4}$$

with $1/(Jg)$ representing the rotor moment of inertia. For $N = 2$ this Hamiltonian has the eigenvalues $Jg\frac{l^2}{2}$ with $l = 0, 1, 2, \ldots$, while for $N = 3$ its eigenvalues are $Jg\frac{l(l+1)}{2}$ with $l = 0, 1, 2, \ldots$.

For a lattice quantum rotor model we combine the kinetic energy with a (ferromagnetic) interaction promoting long-range order, with the result

$$H_R = -J\sum_{\langle ij\rangle}\vec{n}_i \cdot \vec{n}_j + \frac{Jg}{2}\sum_i \vec{L}_i^2 \tag{4.5}$$

As before, the dimensionless parameter g controls the $T = 0$ behavior of the system, and the limits are easily understood:

Limit $g \ll 1$: The dominant interaction leads to an ordered state with $\mathbb{O}(N)$ symmetry broken. Long-range order is described by $|\langle 0|\vec{n}_i|0\rangle| = N_0$ and $\lim_{|\vec{r}_i-\vec{r}_j|\to\infty}\langle 0|\vec{n}_i \cdot \vec{n}_j|0\rangle = N_0^2$.

Limit $g \gg 1$: The dominant kinetic energy leads to a fluctuating, i.e., disordered, phase, with $\langle 0|\vec{n}_i \cdot \vec{n}_j|0\rangle \sim e^{-|\vec{r}_i-\vec{r}_j|/\xi}$.

As a result, a quantum phase transition occurs at an intermediate value of g; this is in the universality class of the $(d+1)$-dimensional classical $\mathbb{O}(N)$ model. We note that

the $T = 0$ ordered phase exists only in spatial dimension $d \geq 2$, as angular fluctuations destroy order otherwise (Mermin-Wagner theorem).[1]

While elementary quantum rotors do not exist in nature, quantum rotors often occur as effective models for low-energy degrees of freedom. For instance, $N = 2$ quantum rotors may capture phase degrees of freedom of superconducting islands, and the lattice model then represents an array of Josephson-coupled islands. $N = 3$ quantum rotors appear in the description of spin models where they can represent degrees of freedom of spin pairs. An explicit example is given by the coupled-dimer model in the next section.

4.3 Coupled-dimer model

The final example is a class of Heisenberg models of spins $\frac{1}{2}$, with the special property that each crystallographic unit cell contains two spins (a "dimer"). We require antiferromagnetic interactions, such that the Hamiltonian reads

$$H = \sum_{\langle ij \rangle} J_{ij} \vec{S}_i \cdot \vec{S}_j, \quad J_{ij} > 0 \tag{4.6}$$

The interactions obey

$$J_{ij} = \begin{cases} J & \text{intradimer bonds} \\ \lambda J & \text{interdimer bonds} \end{cases} . \tag{4.7}$$

As will become clear below, the dimensionless parameter λ controls the quantum phase transition in the system. A sample lattice is shown figure 4.3, where spins live on a square lattice, but the bond strengths are modulated according to Eq. (4.7).

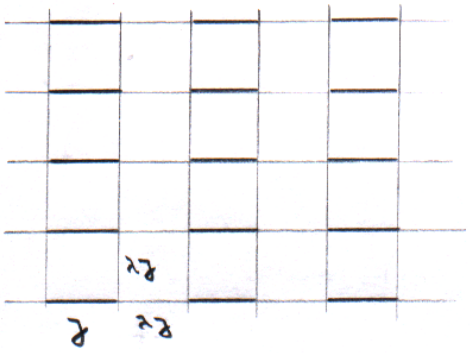

Figure 4.3: Columnar coupled-dimer model on a square lattice: Each unit cell contains two spins connected by a coupling of strength J, while the remaining square-lattice bonds have strength λJ.

The limit $\lambda = 0$ corresponds to disconnected spin pairs, each of them having a singlet $S = 0$ ground state and a triplet $S = 1$ excited state, separated by an excitation energy J. The full lattice model has two distinct phases, which can be easily discussed:

[1] A special case is $d = 1$, $N = 2$, where the ordered phase is replaced by a phase with quasi-long-range order (i.e., a power-law behavior of the correlation function) which is bounded by a Kosterlitz-Thouless transition.

Limit $\lambda \ll 1$: This implies weakly coupled dimers, leading to a disordered (or quantum paramagnetic) phase with no broken symmetries and exponentially decaying spin correlations.

Limit $\lambda \sim 1$: Here the dimers are strongly coupled, and long-range antiferromagnetic order with broken $\mathbb{SU}(2)$ symmetry emerges. (For the lattice shown in Fig. 4.3 $\lambda = 1$ represents a square lattice which is known to display long-range order.)[2]

Again, a quantum phase transition must occur at an intermediate value of λ. As the order parameter is of $\mathbb{O}(3)$ type, the QPT is in the universality class of the $(d+1)$-dimensional classical $\mathbb{O}(3)$ (or Heisenberg) model. The phase diagram is the square-lattice coupled-dimer model of Fig. 4.3 is depicted in Fig. 4.4.

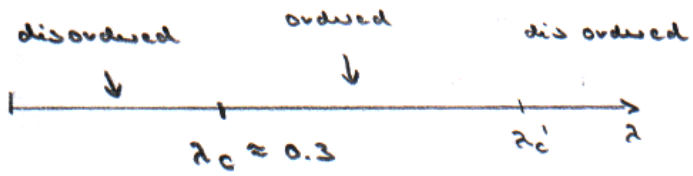

Figure 4.4: Phase diagram for columnar coupled-dimer model of Fig. 4.3.

Coupled-dimer magnets are frequently realized in Mott-insulating materials. Examples are $TlCuCl_3$ [7], a three-dimensional system which can be driven through the QPT by applying pressure, and $BaCuSi_2O_6$ [8] which realizes weakly coupled layers of dimers (i.e. a quasi-two-dimensional system).

[2]The system in Fig. 4.3 becomes disordered again for $\lambda \gg 1$, as this limit corresponds to decoupled spin ladders.

Chapter 5

Quantum phase transitions: Primer

Having illustrated the possibility of phase transitions in the ground state of many-body system, we now turn to a phenomenological description of systems in the vicinity of such phase transitions, in particular at finite temperature. This discussion will also highlight the interplay of quantum and classical fluctuations near QPT.

5.1 Classical and quantum fluctuations

The partition function in a (canonical) Gibbs ensemble,

$$Z = \mathrm{Tr}\left[e^{-\beta \hat{H}}\right] \tag{5.1}$$

factorizes for **classical systems** into kinetic and potential pieces:

$$\begin{aligned} H &= T + V, \\ Z &= \mathrm{Tr}\left[e^{-\beta H}\right] = \mathrm{Tr}\left[e^{-\beta T} e^{-\beta V}\right] \ . \end{aligned}$$

The kinetic energy, $T = \sum_i p_i^2/(2m)$, generically contributes an *analytic* factor to Z because $e^{-\beta T}$ is a product of Gaussian integrals. Hence any non-analyticity in Z, corresponding to a phase transition, can only arise from the potential term $e^{-\beta V}$. For classical systems we conclude:

- Statics and dynamics decouple.
- The exponents listed in Sec. 2.3 (with the exception of z) are determined by the static piece of Z (i.e. the potential V) and constitute a "static" universality class. (Recall: Ginzburg-Landau theory did not involve dynamics.)
- The dynamical exponent z is independent of the other exponents. A given "static" universality class can come with different dynamics.

In contrast, for **quantum systems** the situation is different: In general, $[\hat{T}, \hat{V}]_- \neq 0$. As a result, kinetic and potential part in the partition function do not commute:

$$e^{-\beta H} \neq e^{-\beta T} e^{-\beta V}$$

Therefore statics and dynamics are always coupled, and the dynamical exponent z is integral part of the set of exponents of a given universality class.

Quantum vs. classical transitions: Near any continuous phase transition the correlation length and the correlation time diverge

$$\xi \to \infty \qquad \tau_c \to \infty \tag{5.2}$$

The divergence of τ_c implies the existence of an energy scale $\hbar\omega_c$, representing the typical energy for order-parameter fluctuations, which goes to zero at criticality.

This allows for a sharp distinction between classical and quantum phase transitions: A transition is *classical* if the order-parameter fluctuations follow classical statistical mechanics, i.e., if

$$k_B T_c \gg \hbar\omega_c \,. \tag{5.3}$$

We conclude:

- All phase transitions with $T_c > 0$ are (asymptotically) classical, in the sense that their long-distance fluctuations are in the classical limit. Note that this is not a statement about the physics underlying the ordered state: For instance, the critical behavior of a finite-T transition into a superconducting state is classical, although the physics leading to superconductivity is "quantum".
- for $T_c = 0$, quantum statistics is inevitably needed to describe the order-parameter fluctuations, hence all zero-temperature transitions are quantum in nature.

In a phase diagram spanned by temperature and a non-thermal control parameter, a quantum phase transition is typically the end point of a line of finite-temperature transitions, see figure 5.1(b) below. The criterion (5.3) is fulfilled in a region near the classical transition whose width goes to zero as $T_c \to 0$.

5.2 Phenomenology: Phase diagrams and crossovers

Quantum phase transitions are driven by varying a non-thermal control parameter r at $T = 0$. Experimentally relevant is, of course, the finite-temperature behavior, such that a minimal phase diagram involves the parameters r and T. Schematic phase diagrams of this type, with a continuous quantum phase transition at $r = r_c$, are shown in Fig. 5.1, and we will quickly discuss the main aspects.

The zero-temperature axis features two stable ground states, separated by a quantum critical point at r_c. The low-temperature behavior can be understood by considering the

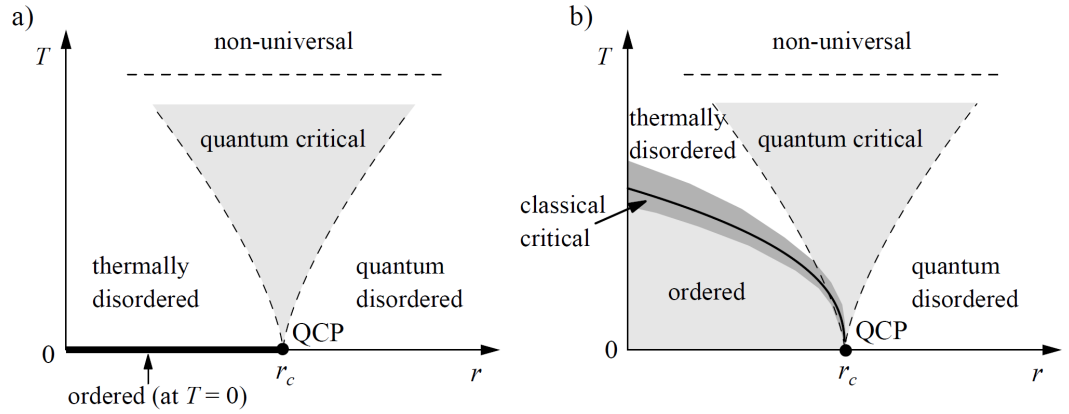

Figure 5.1: Schematic phase diagrams in the vicinity of a quantum critical point (QCP). The horizontal axis represents the control parameter r used to tune the system through the quantum phase transition, the vertical axis is the temperature T. a) Order is only present at zero temperature. The dashed lines indicate the boundaries of the quantum critical region where the leading critical singularities can be observed; these crossover lines are given by $k_B T \sim |r - r_c|^{\nu z}$. b) Order can also exist at finite temperature. The solid line marks the finite-temperature boundary between the ordered and disordered phases. Close to this line, the critical behavior is classical.

elementary excitations on top of the ground state. In the disordered (i.e. non-symmetry-broken) phase, these excitations are typically well-defined quasiparticles with a finite energy gap Δ. The corresponding low-temperature regime will keep the characteristics of the ground state, with an exponentially small density of thermally excited quasiparticles – this is the regime dubbed **quantum disordered**. A similar discussion applies to the ordered side of the QPT, with two complications: (i) Thermal fluctuations may destroy order already at infinitesimal temperature: This applies to Ising systems in $d = 1$ and Heisenberg systems in $d = 2$ and leads to a **thermally disordered** regime at any finite as shown in Fig. 5.1(a). (ii) Even if order survives at finite T, Fig. 5.1(b), there will be no excitation gap in cases with spontaneous breaking of a continuous symmetry. Nevertheless, the density of thermally excited quasiparticles will be small.

This is to be contrasted with the finite-temperature regime, labelled **quantum critical** in Fig. 5.1 and located above the quantum critical point. This regime is bounded by crossover lines $k_B T \sim |r - r_c|^{\nu z}$ (equivalent to $k_B T \sim \Delta$ above a ground state with gap Δ), indicating that pictures of dilute quasiparticle excitations do not apply. Instead, one might think about thermal excitations of the quantum critical ground state. As we will discuss in detail later, the quantum critical state typically does not feature conventional quasiparticles, but a quantum critical continuum of excitations. Thermally exciting this critical continuum leads to unconventional thermodynamic and transport properties in the quantum critical regime, often characterized by fractional temperature exponents. Technically, the quantum critical regime is the universal high-temperature regime of the

field theory underlying the quantum critical point.

In Fig. 5.1(b), where order exists at finite T, there is a finite-temperature transition. According to the discussion above, the critical behavior is classical if $k_B T_c \gg \hbar\omega_c$, which applies to a narrow regime close to the finite-T transition line.

Finally, the behavior far away from criticality, in particular at high temperatures, becomes non-universal. This is the case once the order-parameter correlation length ξ is no longer large – this applies for temperatures $k_B T \gtrsim J$ where J is a representative microscopic energy scale. Numerical simulations have shown that quantum critical behavior in insulating magnets can be observed up to temperatures of $J/3$ where J is the exchange constant [9] – in some systems this may even include room temperature.

5.3 Quantum ϕ^4 theory

As we have seen in the previous chapters, the ϕ^4 (or Ginzburg-Landau) theory is conceptually important in the discussion of critical phenomena. We now construct a quantum version of the classical ϕ^4 theory, the latter given by

$$H = \int d^d x \left(\frac{1}{2}(\partial_i \varphi)^2 + \frac{r}{2}\varphi^2 + \frac{u}{4!}\varphi^4 \right) \tag{5.4}$$

where i runs over x, y, z. In the quantum case, the expression for the partition function needs to be formulated as an imaginary-time path integral,

$$Z = \int \mathfrak{D}[\varphi(r,\tau)] e^{-S} . \tag{5.5}$$

The key new ingredient is a derivative along the (imaginary) time (τ) direction, such that the quantum action is given by

$$S = \int d^d x \int_0^\beta d\tau \left(\frac{c^2}{2}(\partial_i \varphi)^2 + \frac{1}{2}(\partial_\tau \varphi)^2 + \frac{r}{2}\varphi^2 + \frac{u}{4!}\varphi^4 \right) \tag{5.6}$$

and c plays the role of a velocity. Hence, going from classical to quantum essentially amounts to the replacement

$$e^{-\beta H} \to e^{-\int_0^\beta d\tau H} = e^{-S} . \tag{5.7}$$

The form of the time derivative in (5.6) follows – as usual in Ginzburg-Landau theory – from symmetry considerations: In the presence of time-reversal invariance, the quadratic term is the lowest one allowed by symmetry (and higher ones are ignored).

We see that, at $T = 0$ where the imaginary-time axis is infinitely long, the quantum problem in d dimensions is equivalent to the classical problem in $d + z$ dimensions, with the dynamic exponent $z = 1$: Imaginary time enters as z additional space dimensions (compare $\tau_c \sim \xi^z$). In general, z can take any value (including fractional ones), but in

the simple models we have introduced so far (like quantum Ising, quantum rotor etc.) z is locked to unity. This equivalence between quantum problems and classical problems in higher dimensions is known as quantum-to-classical correspondence and will be discussed in more detail later. While this correspondence holds for a number of important models of quantum phase transitions, we note that it breaks down in numerous models of current interest.

The form of the quantum action (5.6) can also be used to discuss the crossover from quantum to classical behavior upon approaching a finite-temperature phase transition. The diverging correlation time τ_c implies that fluctuations along the imaginary-time axis get slow. If $\beta < \infty$, then these fluctuations are effectively frozen once $\tau_c \gtrsim \beta$ – this is equivalent to the condition (5.3). Then, all time dependencies in (5.6) drop out, and the integral over imaginary time can be replaced by a factor β, corresponding to a classical-limit evaluation. For later reference, we note that this reasoning does *not* apply to the quantum critical regime: In this finite-temperature regime, τ_c is of order β, such that thermal and quantum fluctuations are equally important.

5.4 Quantum scaling hypothesis

Recall the classical hypothesis

$$f_s(t,h) = b^{-d} f_s(tb^{y_t}, hb^{y_h}) \tag{5.8}$$

which expresses a homogeneity law for the free-energy density or, alternatively, states how the parameters t and h need to be changed upon a rescaling of lengths in order to restore the physics. It is also useful to remember that this simple form of scaling only applies below the upper critical dimension.

The key difference of the quantum case is that there are now two "directions" which can be used to tune the system away from the zero-temperature critical point, namely the non-thermal control parameter and temperature itself. Hence, f_s acquires T as a new parameter, and we will denote by t the dimensionless distance to criticality on the control-parameter axis, e.g., $t = r - r_c$ or $t = (p - p_c)/p_c$ if the transition is tuned by pressure p. The quantum scaling hypothesis then takes the form

$$f_s(t,h,T) = b^{-(d+z)} f_s(tb^{y_t}, hb^{y_h}, Tb^{y_T}) \tag{5.9}$$

where the exponent $(d+z)$ accounts for the fact that the rescaling factor b acts on both length and time directions, and we work in units where both temperature and field are dimensionless (i.e. measured in suitable microscopic units). As in the classical case, we conclude $y_t = \frac{1}{\nu}$ based on $\xi \propto |t|^{-\nu}$. The definition of the dynamical exponent implies that T scales as

$$\frac{1}{T} \sim (\text{length})^z \longrightarrow y_T = z\,. \tag{5.10}$$

Choosing $b = t^{-\nu}$ yields the scaling relation

$$f_s(t,h,T) = t^{\nu(d+z)} f_s\left(1, \frac{h}{t^{\nu y_h}}, \frac{T}{t^{\nu z}}\right) \tag{5.11}$$

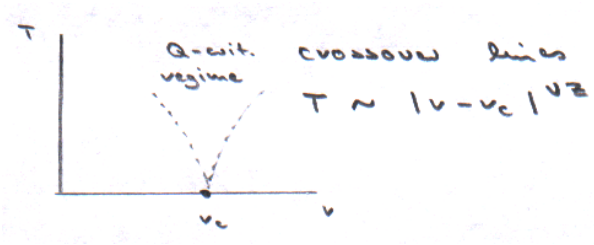

Figure 5.2: Crossover lines at $T \sim |r - r_c|^{\nu z}$

The finite-temperature behavior is controlled by the ratio $T/|t|^{\nu z}$. We distinguish the regimes

$$\frac{T}{|t|^{\nu z}} \begin{cases} \gg 1 & \text{quantum critical regime} \\ \ll 1 & \text{stable-phase regimes} \end{cases} . \tag{5.12}$$

Accordingly, the relation $T \sim |t|^{\nu z}$ defines crossover lines which divide the universal part of the phase diagram in three regimes, Fig. 5.2.

Specializing to the case without external field, $h = 0$, we have

$$\begin{aligned} f_s(t,T) &= t^{\nu(d+z)} f_1\left(\frac{T}{t^{\nu z}}\right) \\ &= T^{(d+z)/z} f_2\left(\frac{T}{t^{\nu z}}\right) \end{aligned}$$

with $f_1(x) = f_2(x) \cdot x^{\nu/z}$. In the quantum critical regime, $t \to 0$, we obtain

$$f_s(t=0,T) = T^{(d+z)/z} \cdot \text{const.} \tag{5.13}$$

This allows to deduce the temperature dependence of (the critical part of) the specific heat as

$$C_{\text{crit}} = VT \frac{\partial^2 f_s}{\partial T^2} \propto T^{d/z} \tag{5.14}$$

exclusively by scaling arguments.[1]

Interestingly, the power-law behavior realized by physical observables upon approaching the QCP either by tuning t or by tuning T can often be related. Consider the entropy S which vanishes at the QCP, but its derivatives are singular. The specific heat C will show power-law behavior, as does the observable $B = \partial S/\partial t$. At a pressure-tuned phase transition, $t = (p - p_c)/p_c$, B measures the thermal expansion,

$$\alpha = \frac{1}{V} \frac{\partial V}{\partial T}\bigg|_p = -\frac{1}{V} \frac{\partial S}{\partial p}\bigg|_T . \tag{5.15}$$

B/C defines the Grüneisen parameter Γ,

$$\Gamma = \frac{\alpha}{C_p} = -\frac{1}{V_m T} \frac{(\partial S/\partial p)_T}{(\partial S/\partial T)_p} \tag{5.16}$$

[1] $C \propto T^{d/z}$ requires hyperscaling and does not necessarily apply above the upper critical dimension.

where $V_m = V/N$ the molar volume. Taking the ratio of the *singular parts* of B and C one observes that the scaling dimensions of T and S cancel, and therefore B/C scales as the inverse of the tuning parameter t. Thus, one obtains a *universal* divergence[2] in the low-T limit [4]

$$\Gamma_{\rm cr}(T=0,t) = \frac{B_{\rm cr}}{C_{\rm cr}} = G_t|t|^{-1}\,, \tag{5.17}$$

$$\Gamma_{\rm cr}(T,t=0) = G_T T^{-1/(\nu z)}\,. \tag{5.18}$$

Given that Γ does not diverge at a finite-T phase transition, a divergence of Γ is a unique signature of a continuous QPT.

5.5 Quantum-to-classical mapping

This section gives deeper insights into the correspondence between quantum phase transitions in d dimensions and classical phase transitions in $(d+1)$ dimensions. We start by establishing the equivalence of the classical Ising spin chain ($d=1$) and the quantum problem of a single spin in a field ($d=0$), valid in the scaling limit of large correlation length. Afterwards, we list more mappings between classical and quantum problems and finally discuss general aspects of the quantum-to-classical correspondence.

5.5.1 Classical Ising chain

We consider the Hamiltonian function of a finite Ising chain,

$$H = -K\sum_{i=1}^{M}\sigma_i^z\sigma_{i+1}^z - h\sum_i \sigma_i^z\,, \tag{5.19}$$

and the parameters K and h are measured in units of the temperature T (formally $T=1$).

Transfer matrix method: The partition function $Z = \sum_{\{\sigma_i\}} e^{-H}$ is

$$Z = \sum_{\{\sigma_i\}}\prod_{i=1}^{M} T_1(\sigma_i^z,\sigma_{i+1}^z)T_2(\sigma_i^z) \tag{5.20}$$

with

$$T_1(\sigma_1^z,\sigma_2^z) = \exp\left(K\sigma_1^z\sigma_2^z\right)$$
$$T_2(\sigma^z) = \exp\left(h\sigma^z\right)$$

[2]For $T\to 0$ even the prefactor G_t is universal and given by a combination of critical exponents.

which is

$$T_1 = \begin{pmatrix} e^K & e^{-K} \\ e^{-K} & e^K \end{pmatrix} , \qquad T_2 = \begin{pmatrix} e^h & 0 \\ 0 & e^{-h} \end{pmatrix} \tag{5.21}$$

where in zero field $h = 0$, $T_2 = 1$. Assuming periodic boundary conditions we get

$$\begin{aligned} Z &= \mathrm{Tr}\,[T_1 T_2 T_1 T_2 \dots] \\ &= \mathrm{Tr}\left[(T_1 T_2)^M\right] \\ &= \mathrm{Tr}\left[(T_2^{\frac{1}{2}} T_1 T_2^{\frac{1}{2}})^M\right] \\ &= \epsilon_1^M + \epsilon_2^M \end{aligned}$$

with the eigenvalues

$$\epsilon_{12} = e^K \cosh(h) \pm \left(e^{2K} \sinh^2(h) + e^{-2K}\right)^{\frac{1}{2}} . \tag{5.22}$$

Correlation function: Restricting ourselves to zero field we have

$$\begin{aligned} \langle \sigma_i^z \sigma_j^z \rangle &= \frac{1}{Z} \sum_{\{\sigma\}} e^{-H} \sigma_i^z \sigma_j^z \\ &= \frac{1}{Z} \left(T_1^i \sigma^z T_1^{j-1} \sigma^z T_1^{M-j} \right) \\ &\vdots \\ &= \frac{\epsilon_1^{M-j+i} \epsilon_2^{j-i} + \epsilon_2^{M-j+i} \epsilon_1^{j-i}}{\epsilon_1^M + \epsilon_2^M} \end{aligned}$$

In the large system limit $M \to \infty$ the correlation function becomes

$$\langle \sigma_i^z \sigma_j^z \rangle = (\tanh K)^{j-i} \tag{5.23}$$

To formulate the scaling limit, it is useful to introducing coordinates $\tau = ja$ where a is the lattice spacing, and to identify $\sigma_j^z \to \sigma^z(\tau)$. The correlation function takes the form

$$\langle \sigma^z(\tau) \sigma^z(0) \rangle = e^{-|\tau|/\xi} \tag{5.24}$$

where ξ is the correlation length, with $1/\xi = \frac{1}{a} \ln \coth K$. At low temperatures $K \gg 1$ we have $\xi/a \sim \frac{1}{2} e^{2K} \gg 1$.

5.5.2 Scaling limit and universality

Universality is made transparent if physical observables are expressed in terms of parameters characterizing the low-energy/long-distance behavior of the system. The present system features the following length scales:

- Large: correlation length ξ, observation scale τ, system size: $L_\tau = Ma$.
- Small: lattice constant a.

The scaling limit is the limit where the ratio of "large" to "small" scales is sent to infinity which is suitable to eliminate microscopic details. Here, we take $a \to 0$ while keeping ξ, τ, L_τ finite. The free-energy density is

$$F = -\frac{\ln Z}{Ma}\,. \tag{5.25}$$

We need the transfer-matrix eigenvalues in the scaling limit

$$\epsilon_{1,2} \sim \left(\frac{2\xi}{a}\right)^{\frac{1}{2}} \left(1 \pm \frac{a}{2\xi}(1 + 4\tilde{h}^2\xi^2)^{\frac{1}{2}}\right) \tag{5.26}$$

where K is expressed using the correlation length ξ, and $\tilde{h} = h/a$. Hence, the free-energy density takes the form

$$F = E_0 - \frac{1}{L_\tau} \ln \left(2\cosh\left(L_\tau \sqrt{\frac{1}{(4\xi)^2} + \tilde{h}^2}\right)\right) \tag{5.27}$$

where the ground state energy at zero temperature is $E_0 = -\frac{K}{a}$. For $\tilde{h} = 0$ the correlation function is

$$\langle \sigma^z(\tau)\sigma^z(0)\rangle = \frac{e^{-|\tau|/\xi} + e^{-(L_\tau - |\tau|)/\xi}}{1 + e^{-L_\tau/\xi}} \tag{5.28}$$

and we recover

$$\langle \sigma^z(\tau)\sigma^z(0)\rangle = e^{-|\tau|/\xi} \tag{5.29}$$

for $L_\tau \gg \xi$.

Universality: Expressions for the observables (expressed in terms $\xi, L_\tau, \tilde{h}$) are identical for all models with the same dimensionality and the same symmetry as H_I, provided that we take the scaling limit $a \to 0$. This can be cast in universal scaling functions. For instance, the for the free-energy density can be written as

$$F = E_0 + \frac{1}{L_\tau}\phi_F\left(\frac{L_\tau}{\xi}, \tilde{h}L_\tau\right) \tag{5.30}$$

with the scaling function $\phi_F(x, y) = -\ln\left(2\cosh\left(\sqrt{(x/2)^2 + y^2}\right)\right)$. Similarly the correlation function can be written as

$$\langle \sigma^z(\tau)\sigma^z(0)\rangle = \phi_\sigma\left(\frac{\tau}{L_\tau}, \frac{L_\tau}{\xi}, \tilde{h}L_\tau\right)\,. \tag{5.31}$$

5.5.3 Mapping to a quantum spin

We now rewrite the partition in a manner suitable to derive a classical-to-quantum correspondence. First, we analyze the transfer matrices T_1 and T_2 in the scaling limit. T_1 can be written as

$$\begin{aligned} T_1 &= e^K(1 + e^{-2K}\sigma^x) \\ &\approx e^K(1 + \frac{a}{2\xi}\sigma^x) \\ &\approx e^{a(-E_0 + \frac{1}{2\xi}\sigma^x)} \end{aligned}$$

at low temperatures where $e^{-2K} \approx a/2\xi$. Also,

$$T_2 = e^{a\tilde{h}\sigma^z} \, . \tag{5.32}$$

The product T_1T_2 can be simplified in the limit $a \to 0$ where

$$e^{a\hat{O}_1}e^{a\hat{O}_2} = e^{a(\hat{O}_1+\hat{O}_2)}(1 + O(a^2)) \tag{5.33}$$

such that

$$T_1T_2 = e^{-a\hat{H}_Q} \tag{5.34}$$

with

$$\hat{H}_Q = E_0 - \frac{\Delta}{2}\sigma^x - \tilde{h}\sigma^z \tag{5.35}$$

and $\Delta = \frac{1}{\xi}$. Then the partition function is

$$Z = \mathrm{Tr}\left[(T_1T_2)^M\right] = \mathrm{Tr}\left[e^{-H_Q/T}\right] \tag{5.36}$$

with $T = \frac{1}{L_\tau}$. This Z apparently represents the partition function of a quantum spin $\frac{1}{2}$ in two perpendicular fields $\tilde{h}$, $\frac{\Delta}{2}$ at a quantum temperature T given by $T = 1/L_\tau$. The free energy

$$F = E_0 - T \ln \left(2 \cosh \frac{1}{T} \sqrt{\frac{\Delta}{4}^2 + \tilde{h}^2} \right) \tag{5.37}$$

is that of a quantum spin in an external field of size $\sqrt{\frac{\Delta}{4}^2 + \tilde{h}^2}$.

Hence, a quantum system at temperature T is equivalent to a classical system of finite length $L_\tau = 1/T$. To make this intuitive, let us consider a small Δ: this implies a small flipping rate for the quantum spin (i.e., a large autocorrelation time) which corresponds to a large correlation length in the classical system. The correspondence between quantum (imaginary) time and classical length is summarized in table 5.1. It is important to realize that in classical systems temperature can always be absorbed by a rescaling of Hamiltonian parameters. In contrast, in a quantum system the temperature is an independent parameter.

Table 5.1: Correspondence between classical spin chain and quantum spin.

classical	quantum
system size L_τ	inverse temperature $1/T$
correlation length ξ	inverse excitation gap Δ

5.5.4 Mapping: XY-chain $\leftrightarrow$ $\mathbb{O}(2)$ quantum rotor

The classical XY-chain can be written by the Hamiltonian

$$H_{cl} = -K \sum_{i=1}^{M} \vec{n}_i \cdot \vec{n}_{i+1} - \sum_{i=1}^{M} \vec{h} \cdot \vec{n}_i \tag{5.38}$$

with $\vec{n}_i^2 = 1$ and $\vec{n}_i = (n_{ix}, n_{iy})$. Using methodology similar to the one above, one can show that this model is equivalent to an $\mathbb{O}(2)$ quantum rotor, with the Hamiltonian

$$H_Q = -\Delta \frac{\partial^2}{\partial \theta^2} - \tilde{h} \cos\theta \,. \tag{5.39}$$

5.5.5 Mapping: Heisenberg chain $\leftrightarrow$ $\mathbb{O}(3)$ quantum rotor

The classical Heisenberg-chain Hamiltonian is similar to the classical XY-chain Hamiltonian

$$H_{cl} = -K \sum_{i=1}^{M} \vec{n}_i \cdot \vec{n}_{i+1} - \sum_{i=1}^{M} \vec{h} \cdot \vec{n}_i \tag{5.40}$$

with $\vec{n}_i^2 = 1$, but now with three-component spins $\vec{n}_i = (n_{ix}, n_{iy}, n_{iz})$. Again, one can shown that this maps onto an $\mathbb{O}(3)$ quantum rotor, described by

$$H_Q = -\frac{\Delta}{2} \hat{\vec{L}}^2 - \tilde{h} \cdot \vec{n} \,. \tag{5.41}$$

It is important to note that the mapping is to a *rotor* instead of a *spin* model: Instead, a quantum spin is characterized by Berry-phase dynamics which has no classical analogue.

5.5.6 Quantum-to-classical correspondence: Rules and exceptions

The previous examples illustrate that certain classes of quantum phase transition in d dimensions correspond to classical transition in $D = d + z$ dimensions. As emphasized before, this correspondence applies to $T = 0$ in the quantum system. It is useful to deduce both thermodynamic properties and correlation functions, and we will employ this in the next chapter. However, it has to be kept in mind that the correspondence is at work on the imaginary time axis of the quantum system, and approximate information on the imaginary axis cannot be easily transformed into approximate information on the real axis, because analytic continuation is an ill-conditioned problem.

More importantly, there are many classes of quantum phase transitions which do *not* obey any quantum-to-classical correspondence. This applies in particular to

- systems with quenched disorder, as disorder is frozen in (imaginary) time;
- systems with quantum or Berry-phase dynamics – such terms are purely imaginary and have no classical analogue. A simple example is the linear-time-derivative describing the dynamics of canonical quantum particles: A single quantum particle has the action

$$S = \phi \partial_\tau \phi - \phi \epsilon_\alpha \phi \tag{5.42}$$

  where $\phi \partial_\tau \phi$ cannot be interpreted classically, see Sec. 7.3.1 for a discussion. Another example are Berry-phase terms describing the dynamics of quantum spins (see the books of Sachdev [1] or Fradkin [3] for spin coherent states).
- systems where a symmetry-breaking order parameter is coupled to low-energy particle-hole pairs of a metal, i.e., quantum phase transitions in metallic or semimetallic systems [10];
- various types of topological phase transitions.

Chapter 6

Magnetic quantum phase transitions

In this chapter we describe in more detail the physics of quantum phase transitions in magnets. We concentrate on insulating magnets, i.e., Mott insulators of local moments; quantum phase transitions in metallic magnets are more complicated due to the interplay between order-parameter fluctuations and low-energy particle-hole pairs [10].

6.1 Order parameters and response functions

We start with a few remarks on order parameters. The definition of a local order parameter φ involves local operator $\hat{O}(\vec{R}_i, t)$ whose thermodynamic average is parameterized as

$$\langle \hat{O}(\vec{R}_i) \rangle = \mathrm{Re}(e^{i\vec{Q}\cdot\vec{R}_i}\varphi(\vec{R}_i)) \tag{6.1}$$

where $\varphi(\vec{R}_i)$ is a slowly varying function of $\vec{R}_i$, which can be a scalar, a vector, tensor, etc. The factor $e^{i\vec{Q}\cdot\vec{R}_i}$ captures possible fast oscillations in the local observable $\hat{O}$, for instance he up–down oscillation of the magnetization in an antiferromagnet (i.e. staggered magnetization). $\vec{Q}$ is called the ordering wavevector, and $e^{i\vec{Q}\cdot\vec{R}_i}$ must be chosen such that $\varphi(\vec{R}_i)$ varies slowly on the lattice scale.

Examples for ordered states are

- Charge density wave (CDW):

$$\langle \hat{\rho}(\vec{R}) \rangle = \rho_0 + \mathrm{Re}(e^{i\vec{Q}\cdot\vec{R}_i}\varphi_C(\vec{R})) \tag{6.2}$$

  where φ has $N = 1$ components.

- Spin density wave (SDW):

$$\langle \hat{S}_\alpha(\vec{R}) \rangle = \mathrm{Re}(e^{i\vec{Q}\cdot\vec{R}_i}\varphi_{S\alpha}(\vec{R})) \tag{6.3}$$

  where φ has $N = 3$ components.

If $\vec{Q} = 0$ then the order parameter is real, otherwise φ can be complex. Exceptions are, e.g., on the cubic lattice with $\vec{Q} = (\pi, \pi, \pi)$, where $e^{i\vec{Q}\cdot\vec{R}_i}$ is real for all $\vec{R}_i$. In general, the phase of a complex φ takes discrete values if $\vec{Q}$ is commensurate with the lattice, i.e. the ratio of $\vec{Q}$ and the lattice constant is a rational number.

For spin density waves, different modulation types are possible due to the vector character of the order. One class, with all $\langle\vec{S}\rangle$ pointing along the same axis, is dubbed collinear and shown in figure 6.1. A proper parametrization of the corresponding order

Figure 6.1: Collinear arrangement of spins

parameter is $\varphi_{S\alpha} = e^{i\theta} n_\alpha$ with n_α real.[1] A second class are spiral states as shown in figure 6.2. Here the order parameter is $\varphi_{S\alpha} = n_{1\alpha} + i n_{2\alpha}$ with $n_{1,2\alpha}$ real and $\vec{n}_1 \cdot \vec{n}_2 = 0$.

Figure 6.2: Spiral (non-collinear) arrangement of spins

Experiments typically observe correlation functions of the order parameter; for magnets this can be done for instance using magnetic neutron scattering. We now define the most important correlation and response functions to be discussed below.

We start with a real-time correlation function

$$C(\vec{r}, t; \vec{r}', t') = \langle \varphi(\vec{r}, t) \varphi(\vec{r}', t') \rangle \tag{6.4}$$

where $\langle \ldots \rangle = (1/Z)\mathrm{Tr}\left[e^{-\beta H} \ldots\right]$ is the thermodynamic average. Its Fourier transform yields the dynamic structure factor

$$S(\vec{k}, \omega) = \int d^d r \int_{-\infty}^{\infty} dt C(\vec{r}, t; 0, 0) e^{-i\vec{k}\cdot\vec{r} + i\omega t} \tag{6.5}$$

where translation invariance in space and time has been assumed. In addition, it is useful to consider an imaginary-time correlation function

$$C(\vec{r}, \tau; \vec{r}', \tau') = \langle \hat{T}_\tau \varphi(\vec{r}, \tau) \varphi(\vec{r}', \tau') \rangle \tag{6.6}$$

where $\hat{T}_\tau$ is the time-ordering operator on the imaginary-time axis. This can be used to define a dynamic susceptibility

$$\chi(\vec{k}, i\omega_n) = \int d^d r \int_0^{1/T} d\tau C(\vec{r}, \tau; 0, 0) e^{-i\vec{k}\cdot\vec{r} + i\omega_n \tau} \tag{6.7}$$

[1] θ denotes sliding degree of freedom for a density wave.

where $\omega_n = 2\pi n T$ are called (bosonic) Matsubara frequencies, and we recall that the imaginary-time correlator is periodic in time with period $1/T$. The **fluctuation-dissipation theorem**, which can be derived via the spectral representation of the correlation functions, states that

$$S(\vec{k},\omega) = \frac{2}{1-e^{-\omega/T}} \mathrm{Im}\chi(\vec{k},\omega) \tag{6.8}$$

where $\mathrm{Im}\chi(\vec{k},\omega)$ has been obtained from the imaginary-frequency dynamic susceptibility by analytic continuation.[2] Note that $\mathrm{Im}\chi(\vec{k},\omega)$ is also called the spectral density.

6.2 Properties of the quantum ϕ^4 model

We now discuss a few observable properties of systems described by the quantum ϕ^4 model:

$$S = \int d^d x \int_0^\beta d\tau \left(\frac{c^2}{2}(\partial_i \varphi)^2 + \frac{1}{2}(\partial_\tau \varphi)^2 + \frac{r}{2}\varphi^2 + \frac{u}{4!}\varphi^4 \right) \tag{6.9}$$

Zero-temperature properties can be deduced from the classical results, discussed in Chapters 2 and 3, via the quantum-to-classical (here: classical-to-quantum) correspondence. The present model has a dynamical exponent of $z = 1$, hence the mapping is from $(d+1)$ space dimensions to d space and one (imaginary) time dimension: $|\vec{k}| \leftrightarrow (c^2\vec{k}^2 + (i\omega)^2)^{1/2}$ where a velocity factor has been added. This implies that at criticality the dynamical two-point correlation function is given by

$$\chi(k,\omega) \propto \frac{1}{(c^2k^2 - (\omega + i\delta)^2)^{1-\eta/2}} \,. \tag{6.10}$$

This is the advertised critical continuum of excitations, Fig. 6.3: Above a threshold given by $\omega = ck$ this function has branch cuts instead of poles, hence quasiparticles are absent for $\eta \neq 0$.[3]

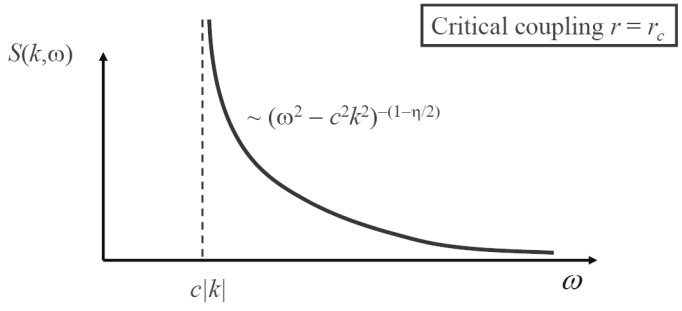

Figure 6.3: Dynamic structure factor $S(k,\omega) \propto \mathrm{Im}\chi(k,\omega)$ at the critical point, displaying a critical continuum of excitations.

[2] Technically, $\chi(\vec{k},\omega)$ is a retarded Green's function which requires an analytic continuation $i\omega_n \leftrightarrow \omega + i\delta|_{\delta\to 0}$.

[3] The quantum critical response (6.10) displays quasiparticle poles for $\eta = 0$. In cases where η is non-zero but numerically small the critical continuum is difficult to distinguish experimentally from conventional quasiparticle response.

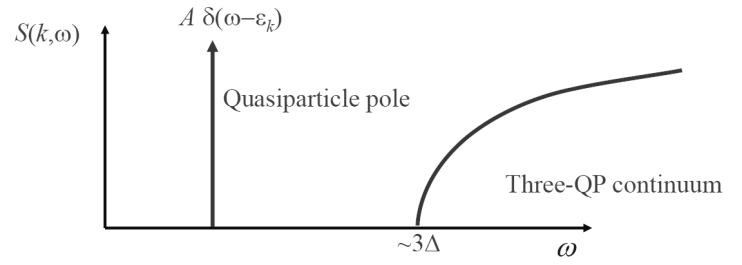

Figure 6.4: Dynamic structure factor in the disordered phase.

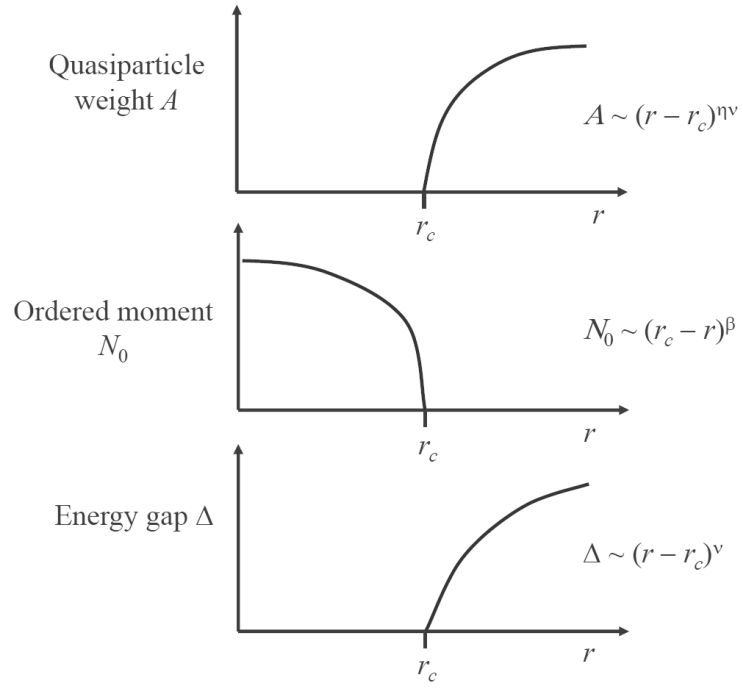

Figure 6.5: Evolution of the quasiparticle weight and the energy gap in the disordered phase as well as the order parameter in the ordered phase as function of the control paramter r of a quantum phase transition.

Away from criticality in the disordered phase we have

$$\chi(k,\omega) = \frac{1}{c^2k^2 + r - (\omega + i\delta)^2) - \Sigma(k,\omega)} \tag{6.11}$$

where $\Sigma(k,\omega)$ contains the contributions from the quartic coupling. Away from criticality, Σ is non-singular, and $\chi(k,\omega)$ will display quasiparticle poles:

$$\mathrm{Im}\chi(k,\omega) = \frac{\mathcal{A}}{2\epsilon_k}\left(\delta(\omega - \epsilon_k) - \delta(\omega + \epsilon_k)\right) \tag{6.12}$$

where $\epsilon_k^2 = c^2k^2 + r - \Sigma$ refers to the quasiparticle dispersion. The role of Σ is to modify both dispersion and the pole weight $\mathcal{A}$ (but not to remove the pole). The energy position of the pole at $k = 0$ defines the energy gap, $\Delta^2 = r - \Sigma(k = 0, \omega = \Delta)$, and the dispersion near $k = 0$ can be parameterized as $\epsilon_k = \Delta + c^2k^2/(2\Delta)$. At higher energies, scattering processes induce n-particle continua in $\mathrm{Im}\chi(k,\omega)$ with $n = 3, 5, 7, \ldots$, see Fig. 6.4.

Near criticality, one may cast the $T = 0$ susceptibility into the scaling form

$$\chi(k,\omega) = \frac{1}{\Delta^{2-\eta}} f_\chi\left(\frac{ck}{\Delta}, \frac{\omega}{\Delta}\right) \tag{6.13}$$

which shows that the weight of the single-particle pole scales as $\mathcal{A} \propto \Delta^\eta$.

On the magnetically ordered side, the structure factor displays a Bragg peak

$$S(k,\omega) = N_0^2 (2\pi)^{d+1} \delta(\omega)\delta(k) + \ldots \tag{6.14}$$

where the dots represent finite-frequency contributions. For $N > 1$ the transverse susceptibility displays poles from gapless Goldstone modes, while the longitudinal susceptibility is generically gapped – it shows a damped by well-defined mode near criticality which is often dubbed amplitude or Higgs mode.

Fig. 6.5 illustrates some of the results collected above, for a discussion of finite-temperature results we refer the reader to the literature [1].

6.3 Quantum Ising chain

After having discussed general properties of the continuum ϕ^4 model, we now supplement this by similar considerations for the quantum Ising chain, i.e., the model described in Sec. 4.1 in $d = 1$. This is a microscopic model which can be essentially solved exactly, and allows to obtain concrete results which are consistent with the general phenomenology discussed above. We consider the Hamiltonian

$$H_I = -J \sum_i (g\sigma^x + \sigma_i^z \sigma_{i+1}^z) \tag{6.15}$$

which we will first examine at both strong coupling, $g \gg 1$, and weak coupling, $g \ll 1$.

6.3.1 Strong-coupling limit $g \gg 1$

When

$g = \infty$**:** the ground state is $|\Psi_0\rangle = \prod_i |{\rightarrow}\rangle_i$, where $|{\rightarrow}\rangle$ denotes an eigenstate of σ_x.

$g < \infty$**:**

$$|\Psi_0\rangle = \prod_i |{\rightarrow}\rangle_i - \frac{1}{2g} \sum_i |\cdots {\rightarrow}{\leftarrow}_i {\leftarrow}_{i+1} {\rightarrow}{\rightarrow} \ldots\rangle - \ldots \tag{6.16}$$

which means that $C(x,0) \sim e^{-x/\xi}$ (a disordered phase).

One-particle excitations: In the cases

$g = \infty$**:** the first excited state is $|i\rangle = |{\leftarrow}\rangle_i \prod_{j\neq i} |{\rightarrow}\rangle_j$ with $\epsilon = 2gJ$.

$g < \infty$**:** then $|k\rangle = \frac{1}{\sqrt{N}} \sum_j e^{ikx_j} |j\rangle$ with $\epsilon_k = gJ(2 - \frac{2}{g}\cos ka + O(\frac{1}{g^2}))$. For this dispersion relation see figure 6.6.

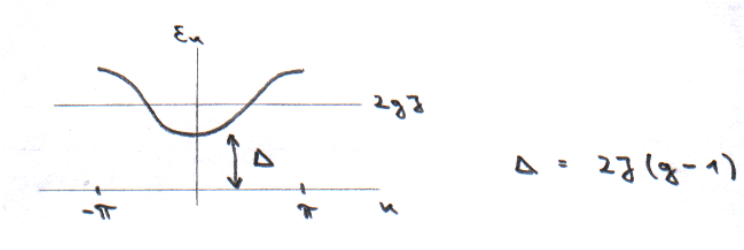

Figure 6.6: Dispersion of single-spin-flip excitations of the quantum Ising chain in the strong-coupling limit.

Two-particle excitations

$g = \infty$**:** then $|ij\rangle = |\leftarrow\rangle_i |\leftarrow\rangle_j \prod_{l\neq i,j} |\rightarrow\rangle_l$

$g < \infty$**:** when far apart, particles are independent, when close together, they scatter. For details see Sachdev's book.

Dynamic structure factor at $T = 0$ is

$$S(k,\omega) = 2\pi \sum_{|\Psi_\alpha\rangle} |\langle\Psi_\alpha| \sigma^z |\Psi_0\rangle|^2 \delta(\omega - E_\alpha) \tag{6.17}$$

see figure 6.7.

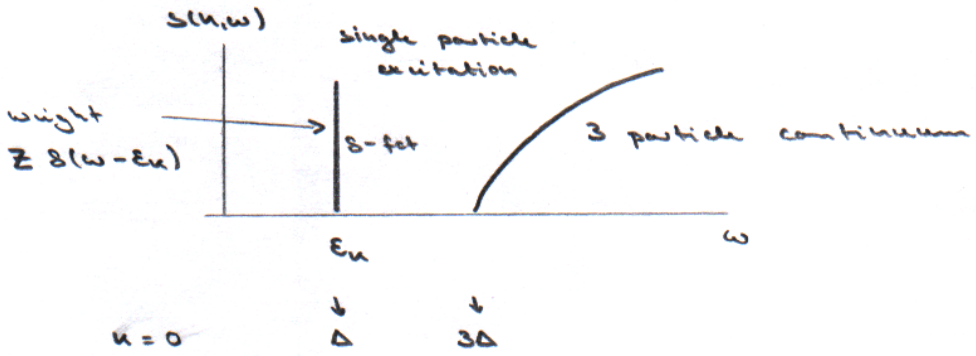

Figure 6.7: Dynamic structure factor of the quantum Ising chain in the strong-coupling limit.

6.3.2 Weak-coupling limit $g \ll 1$

The system is in the ordered phase at $T = 0$, which is implied by

$$\lim_{|x|\to\infty} C(x,0) = N_0^2 \neq 0 \tag{6.18}$$

The ground state is

for $g = 0$

$$|\Psi_0\rangle = \begin{cases} \prod_i |\uparrow\rangle_i \\ \prod_i |\downarrow\rangle_i \end{cases} \tag{6.19}$$

and for $g > 0$

$$|\Psi_0\rangle = \prod_i |\uparrow\rangle_i - \frac{g}{2} \sum_i |\ldots\uparrow\downarrow_i\uparrow\uparrow\ldots\rangle - \ldots \tag{6.20}$$

One-particle excitation, if

$g = 0$, is $|i\rangle = |\ldots\uparrow\downarrow_i\downarrow\downarrow\ldots\rangle$, with $\epsilon = 2J$, where at i the particle is the domain wall.

$g > 0$, is $|k\rangle = \frac{1}{\sqrt{N}} \sum_i e^{ikx_i} |i\rangle$ with $\epsilon_k = J(2 - 2g\cos ka) + O(g^2)$, see figure 6.8

Figure 6.8: Dispersion of domain-wall excitations of the quantum Ising chain in the weak-coupling limit.

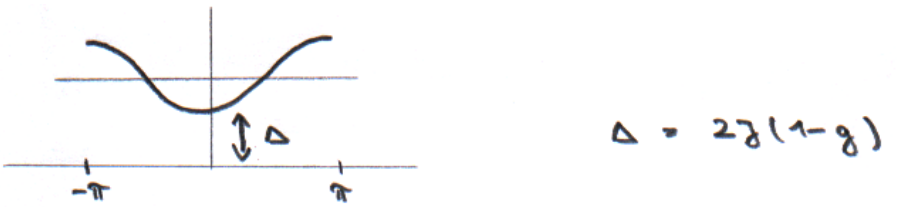

Dynamic structure factor. There are two special things to note:

- We have an ordered phase, which gives a Bragg peak at $k = 0$ and $\omega = 0$.
- We are in 1D, thus we can only create 2 domain walls at a time, thus the one particle peak is absent in 1D.[4]

See figure 6.9.

6.3.3 Exact spectrum

Representing spins by fermions by the *Jordan-Wigner transformation*

$$\begin{aligned} \sigma_i^z &= 1 - 2c_i^\dagger c_i \\ \sigma_i^+ &= \prod_{j<i} (1 - 2c_j^\dagger c_j) c_i \\ \sigma_i^- &= \prod_{j<i} (1 - 2c_j^\dagger c_j) c_i^\dagger \end{aligned}$$

[4] In higher dimensions, the elementary excitations of the ordered phase would be spin flips instead of domain walls, resulting in a single-particle peak in the dynamic structure factor.

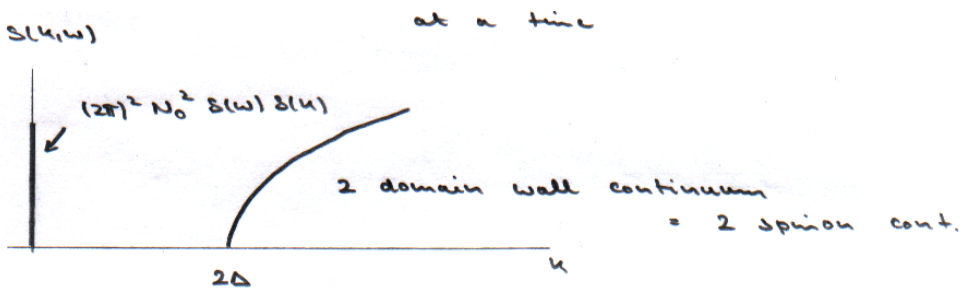

Figure 6.9: Dynamic structure factor of the quantum Ising chain in the weak-coupling limit.

where the factor $\prod_{j<i}(1-2c_j^\dagger c_j)$ counting the number of fermions to the left ensures anticommutation rules of the fermions on different sites, while spins on different sites have commutation rules. The inverse transformation is

$$c_i = (\prod_{j<i}\sigma_j^z)\sigma_i^+$$
$$c_i^\dagger = (\prod_{j<i}\sigma_j^z)\sigma_i^-$$

The transformation is not local! Applying this to quantum Ising chain rotated by 90° gives

$$\sigma_i^x = 1 - 2c_i^\dagger c_i$$
$$\sigma_i^z = -\prod_{j<i}(1-2c_j^\dagger c_j)(c_i + c_i^\dagger)$$

and plugging into the Hamiltonian

$$H_I = -J\sum_i (c_i^\dagger c_{i+1} + c_{i+1}^\dagger c_i + c_i^\dagger c_{i+1}^\dagger + c_{i+1}c_i - 2gc_i^\dagger c_i + g) \tag{6.21}$$

after Fourier transform we have

$$H_I = J\sum_k \Big(2(g-\cos ka)c_k^\dagger c_k - i\sin ka(c_{-k}^\dagger c_k^\dagger + c_{-k}c_k - g)\Big) \tag{6.22}$$

A Bogoliubov transformation

$$\gamma_k = u_k c_k - iv_k c_{-k}^\dagger$$
$$c_k = u_k\gamma_k + iv_k\gamma_{-k}^\dagger$$

with $u_k^2 + v_k^2 = 1$, $u_{-k} = -u_k$ and $v_{-k} = -v_k$ correctly chosen, gets rid of the anomalous terms. The correct choice (with parameter θ defined by $u_k = \cos\theta_k/2, v_k = \sin\theta_k/2$) is

$$\tan\theta_k = \frac{\sin ka}{\cos ka - g}\,. \tag{6.23}$$

The diagonalized Hamiltonian takes the form:

$$H_I = \sum_k \epsilon_k (\gamma_k^\dagger \gamma_k - \frac{1}{2}) \,, \tag{6.24}$$

$$\epsilon_k = 2J(1 + g^2 - 2g \cos ka)^{\frac{1}{2}} \geq 0 \,. \tag{6.25}$$

Given that $\epsilon_k = 0$ only for $g = 1$ and $k = 0$, we conclude that we have a quantum critical point at $g = 1$. The dispersion minimum near the critical point obeys

$$\Delta \equiv \epsilon_{k=0} = 2J|1 - g| \tag{6.26}$$

from which we conclude $\nu z = 1$.

The exact solution can now be used to calculate correlation functions, structure factor, etc. see Sachdev's book [1]. We note a remarkable aspect of the solution: The form (6.24) shows no obvious signature of spontaneous symmetry breaking, and the qualitative distinction between the two phases appears lost. In fact, the physics is hidden in the Bogoliubov transformation together with the non-local character of the Jordan-Wigner transformation. We further note that the two phases of the quantum Ising chain can be mapped onto each other by a suitable duality transformation which exchanges $g \leftrightarrow 1/g$ – this is consistent with Eq. (6.26).

6.3.4 Results near criticality

The results for the excitation gap, the ferromagnetic moment (the order parameter) and the flipped-spin quasiparticle weight are shown in figures 6.10 and 6.11

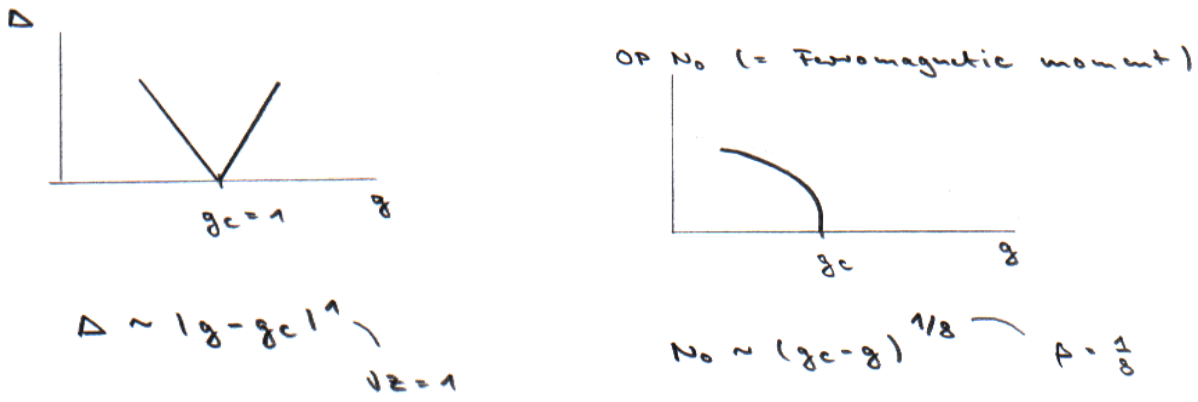

Figure 6.10: Excitation gap and ferromagnetic moment (order parameter) of the quantum Ising chain near criticality.

The exact solution might suggest that there are well-defined quasiparticles (spin flips or domain walls) even at the critical point $g = 1$, but this is incorrect:[5] The

[5]The non-local character of the Jordan-Wigner transformation is responsible for the non-trivial behavior of physical observables.

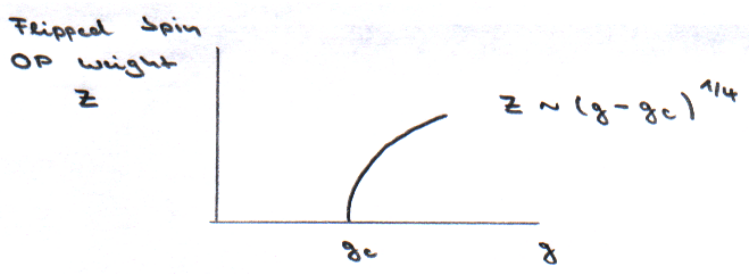

Figure 6.11: Flipped-spin quasiparticle weight in the disordered phase of the quantum Ising model.

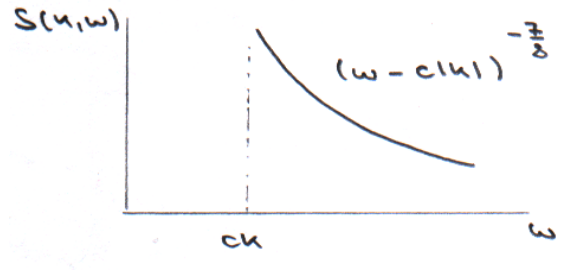

Figure 6.12: Dynamic structure factor of the quantum Ising model at criticality.

structure factor, Fig. 6.12, displays a dissipative critical continuum instead, consistent with the general arguments made previously. To understand how the structure evolves from its strong-coupling form, Fig. 6.7, to the quantum critical form, we note (i) both the weight of the quasiparticle peak and its energy location go to zero upon approaching the critical point, $Z \to 0$, $\Delta \to 0$. Further, $\Delta \to 0$ also implies that all multi-particle continua move towards zero energy, and their superposition results in the critical power law $(\omega - c|k|)^{-7/8}$. This is illustrated in Fig. 6.13 which shows the structure factor for g slightly above $g_c = 1$.

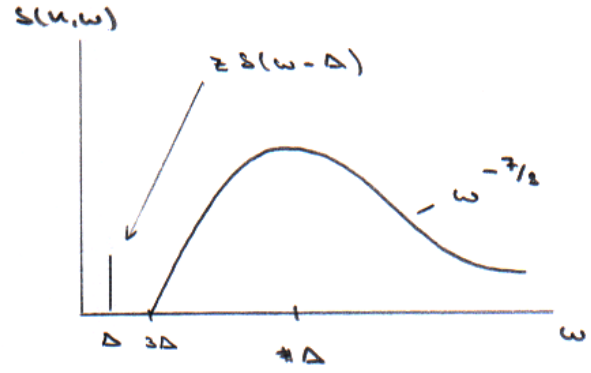

Figure 6.13: Dynamic structure factor in the disordered phase very close to criticality.

The structure of the ground states and elementary excitations derived so far allows to deduce the finite-temperature phase diagram, see Fig. 6.14. Finally we note that non-universal physics takes over at large T where ξ is no longer large but becomes comparable to the lattice constant a.

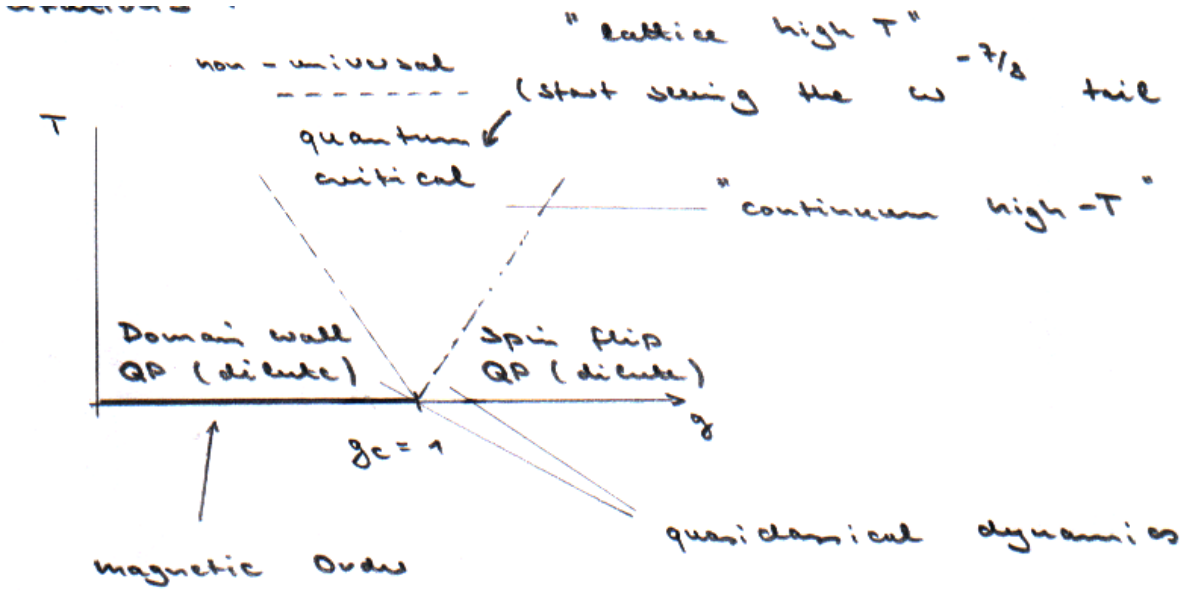

Figure 6.14: Finite-temperature phase diagram of the quantum Ising chain.

Chapter 7

Quantum phase transitions of bosons and fermions

In this last chapter we turn to quantum phase transitions where the dynamics of quantum particles plays a role (as opposed to those with collective density fluctuations only).

7.1 Bose-Hubbard model

We start by considering a microscopic model of bosons on a lattice which interact via an on-site density-density interaction:

$$H = -w \sum_{\langle ij \rangle} \left(b_i^\dagger b_j + \text{h.c.} \right) - \mu \sum_i n_i + \frac{1}{2} U \sum_i n_i (n_i - 1) \tag{7.1}$$

with w being a hopping matrix element and U the strength of the interaction. This model is known as the Bose-Hubbard model. It applies to systems of charge-neutral bosons with contact interactions, as realized for helium atoms adsorbed on surfaces (like graphite) or for ultra-cold bosonic atoms on optical lattices.

Let us discuss the behavior in the low-temperature limit: First, non-interacting bosons ($U/w = 0$) form a Bose-Einstein condensate, with all particles condensed at $T = 0$. Weak interactions ($U/w \ll 1$) turn this condensate into a proper superfluid with phase stiffness, but also reduce the condensate fraction. Strongly interacting lattice bosons can, in general, host a variety of non-trivial phases. For the simple model in Eq. (7.1), however, the only other $T = 0$ phase is a **Mott insulator** – this phase exists at strong interactions, $U/w \gg 1$, and integer filling $\langle n \rangle$. It is characterized by bosons being localized on lattice sites, with number fluctuations being suppressed.[1]

The model (7.1) can be conveniently realized for ultracold bosonic atoms in the presence of a periodic potential arising from an optical lattice. Figures 7.1 and 7.2

[1] Note that the Mott insulator is a genuine *lattice* phase whereas the superfluid can exist in a continuum system as well.

illustrate the lattice potential, with modulation amplitude v. Small v will lead to large w,[2] and the system will be a superfluid. Large v leads to small w: Here the system is a Mott insulator for integer densities, whereas for non-integer (incommensurate) densities, $\langle n \rangle \sim 1 + \delta n$, extra particles are mobile such that a superfluid with a condensate density $\sim \delta n$ emerges.

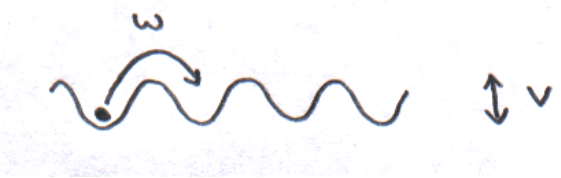

Figure 7.1: Bosons in a shallow potential (implying $U/w \ll 1$): The ground state is generically superfluid.

Figure 7.2 shows a deep potential.

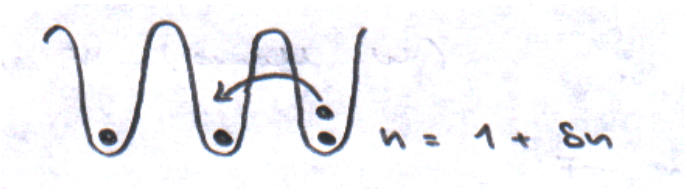

Figure 7.2: Bosons in a deep potential (i.e. $U/w \gg 1$): The ground state is superfluid for non-integer densities.

7.2 Bose-Hubbard model: Mean-field theory

We now describe a simple mean-field theory which captures both the superfluid and the Mott insulator phase. Given that the Mott insulator is featureless whereas the superfluid breaks a $\mathbb{U}(1)$ symmetry, it is useful to introduce an order parameter for the condensate:

$$\Psi_B = zw\langle b_i \rangle \qquad (b_i = \frac{1}{zw}\Psi_B + \delta b_i) \tag{7.2}$$

where z is the number of nearest neighbor on the lattice (i.e. coordination number). This order parameter is used to decouple the kinetic-energy term (!). Then the mean-field Hamiltonian is purely local:

$$H_{\mathrm{MF}} = \sum_i \left(-\mu n_i + \frac{1}{2} U n_i (n_i - 1) - \Psi_B^\star b_i - \Psi_B b_i^\dagger \right) + \text{const.} \tag{7.3}$$

The possible mean-field phases are:

[2]For a shallow potential, higher Bloch bands not described by Eq. (7.1) might play a role.

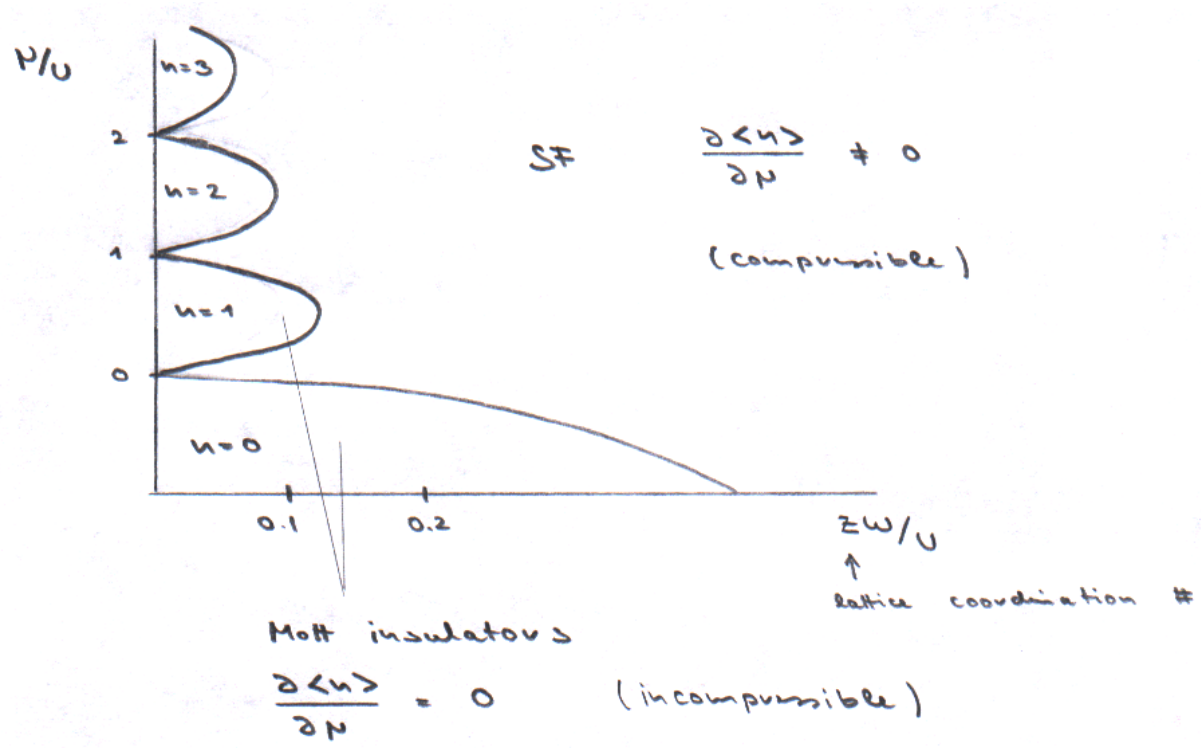

Figure 7.3: Mean-field phase diagram of the Bose-Hubbard model as function of μ/U and zw/U, showing Mott and superfluid phases.

- $\Psi_B \neq 0$: superfluid, which breaks the $\mathbb{U}(1)$ phase symmetry $\Psi_B = |\Psi_B|e^{i\phi}$, with the condensate phase ϕ.
- $\Psi_B = 0$: Mott insulator, with no kinetic energy at the mean-field level.

Then the mean-field ground state energy E_{MF} is calculated, by minimizing E_{MF} w.r.t. Ψ_b. In general this has to be done numerically, but the case $w \to 0$ can be analyzed easily: This always yields a Mott insulator having exactly n_0 particles per site, with μ and U determining n_0:

$$n_0 = \begin{cases} 0 & \text{for} \quad \mu/U < 0 \\ 1 & \text{for} \quad 0 < \mu/U < 1 \\ 2 & \text{for} \quad 1 < \mu/U < 2 \\ \vdots \end{cases} \tag{7.4}$$

Figure 7.3 shows the mean-field phase diagram, μ/U as a function of zw/U. The superfluid phase is compressible with $\partial\langle n\rangle/\partial\mu \neq 0$. The Mott insulator phase is incompressible with $\partial\langle n\rangle/\partial\mu = 0$. This mean-field phase diagram has been checked and confirmed by Monte Carlo simulations, and mean-field theory has been shown to be qualitatively (and even semi-quantitatively) correct.

7.3 Superfluid-insulator transition: Field theory

We now turn to discuss the quantum phase transition between Mott insulator and superfluid in more detail. It turns out that the behavior of the boson density play a key role. This density is fixed in each Mott insulator phase, but varies continuously in the superfluid phase. This is illustrated in Figure 7.4 which shows lines of constant density.

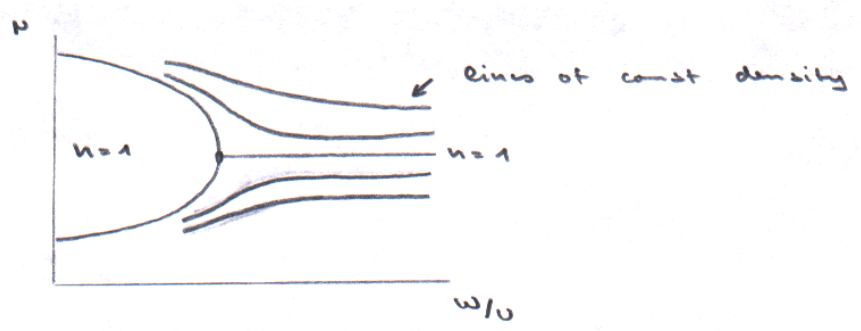

Figure 7.4: Lines of constant boson density $\langle n \rangle$ in the phase diagram of the Bose-Hubbard model.

As we will derive below, there exist two distinct universality classes for the Mott–superfluid quantum phase transiton:

- If the density is constant across the transition (this applies to the tip of the Mott lobe, as derived below), the critical fluctuations are phase fluctuations of the condensate, and consequently the transition is that of an $\mathbb{O}(2)$ rotor model.
- If density varies across the transition (away from the Mott lobe), both condensate phase and density are critical. The corresponding critical theory will be derived now.

We start from a path-integral representation of the Bose-Hubbard model:

$$Z_B = \int \mathfrak{D}[b_i(\tau)]\mathfrak{D}[b_i^\star(\tau)] \exp\left(-\int_0^{1/T} \mathfrak{L}_B\right) \tag{7.5}$$

$$\mathfrak{L}_B = \sum_i \left(b_i^\star \frac{\partial b_i}{\partial \tau} - \mu b_i^\star b_i + \frac{1}{2} U b_i^\star b_i (b_i^\star b_i - 1) - w \sum_{\langle ij \rangle} (b_i^\star b_j + \text{c.c.}) \right) \tag{7.6}$$

Introduce an auxiliary field $\psi_{B_i}(\tau)$ via Hubbard-Stratonovich transformation of the *hopping* term, which eliminates the non-local term. Then

$$Z_B = \int \mathfrak{D}[b_i(\tau)]\mathfrak{D}[b_i^\star(\tau)]\mathfrak{D}[\psi_B]\mathfrak{D}[\psi_B^\star] \exp\left(-\int_0^{1/T} \mathfrak{L}'_B\right) \tag{7.7}$$

with the new Lagrangian

$$\mathfrak{L}'_B = \sum_i \left(b_i^\star \frac{\partial b_i}{\partial \tau} - \mu b_i^\star b_i + \frac{1}{2} U b_i^\star b_i (b_i^\star b_i - 1) - \psi_{B_i} b_i^\star - \psi_{B_i}^\star b_i \right) + \sum_{\langle ij \rangle} \psi_{B_i}^\star w_{ij}^{-1} \psi_{B_j} \quad (7.8)$$

where

$$w_{ij} = \begin{cases} w & \text{if } i,j \text{ are neighbors} \\ 0 & \text{otherwise} \end{cases} \quad (7.9)$$

Now we integrate out the b field – this is possible since the terms are all local – and arrive at an action for the ψ_B alone,

$$Z_B = \int \mathfrak{D}[\psi_B] \mathfrak{D}[\psi_B^\star] \exp\left(- \int d\tau \mathfrak{L}''_B - F_0/T \right), \quad (7.10)$$

with F_0/T being the constant arising from the transformation. Instead of explicitly deriving the action for ψ_B, we guess the result by writing down all the terms allowed by symmetry. This yields:

$$Z_B = \int D\Psi_B D\Psi_B^\star e^{-S''} \quad (7.11)$$

$$S'' = \int d^d x \int d\tau \left(K_1 \Psi_B^\star \frac{\partial \Psi_B}{\partial \tau} + K_2 \left| \frac{\partial \Psi_B}{\partial \tau} \right|^2 + r \left| \Psi_B \right|^2 + K_3 \left| \nabla \Psi_B \right|^2 + \frac{1}{2} U |\Psi_B|^4 + \cdots \right) \quad (7.12)$$

where r is the control parameter of the theory. Here we have included both a linear and a quadratic time derivative, which we analyze now. To this end, we note that $\mathfrak{L}'_B$ is invariant under the $\mathbb{U}(1)$ gauge transformation:

$$b_i \to b_i e^{i\phi(\tau)}$$
$$\psi_{B_i} \to \psi_{B_i} e^{i\phi(\tau)}$$
$$\mu \to \mu + i \frac{\partial \phi}{\partial \tau}$$

Demanding that $\mathfrak{L}''_B$ is also invariant under this transformation gives

$$K_1 = -\frac{\partial r}{\partial \mu} \quad (7.13)$$

i.e., the linear-time-derivative term is present only if $\partial r / \partial \mu$ is non-vanishing.

7.3.1 Quadratic vs. linear time derivative

The theory (7.11) can have two qualitatively distinct low-energy behaviors, depending on whether or not K_1 is finite. (i) For $K_1 = 0$ there is a quadratic time derivative only,

as in the quantum ϕ^4 theory. From Eq. (7.13) we see that $K_1 = 0$ applies to the tip of the Mott lobe where the transition occurs with at fixed density $\langle n \rangle$. Consequently, this transition is that of an $\mathbb{O}(2)$ ϕ^4 theory, or, equivalently, of an $\mathbb{O}(2)$ rotor model. The critical variable is the phase of the condensate (and the density is fixed). (ii) For $K_1 \neq 0$, away from the tips of the Mott lobes, a linear time derivative is present which dominates at low energies over the quadratic one. Hence, the critical theory is different: As we will see below, the density itself becomes a critical degree of freedom, and the transition does not have a straightforward quantum-to-classical correspondence. A detailed discussion of the transition follows in Section 7.4.

Having realized that the order of time derivative is crucial in determining quantum critical properties, let us recall where these time derivatives arise from: In the quantum ϕ^4 theory the quadratic time derivative is dictated from the gradient expansion, combined with demanding time-reversal invariance, for the order-parameter field theory. The linear time derivative instead can be traced back to the dynamics of canonical quantum particles which genuinely has a time direction. Phrased differently, for a quantum particles forward and backward propagation need to be distinguished (recall that Feynman diagrams have arrows). However, for hermitian objects (like order-parameter fields) propagators have no time arrow – in a sense, their propagators are sums of forward and backward processes. This can be nicely seen by thinking about harmonic oscillators, phonons, and the like: The Hamiltonian is written in terms of canonical bosons, and their propagators are directed. In contrast, both position and momentum operators are hermitian, and their propagators are undirected. A critical theory involving these variables only would be of ϕ^4 type, with quadratic time derivative.

7.4 Dilute Bose gas

We continue by studying a model of weakly interacting bosons with a chemical potential near zero, describing a dilute gas of bosons:

$$H_B = \sum_k \frac{k^2}{2m} b_k^\dagger b_k - \sum_k \mu n_k + U \sum_i n_i (n_i - 1) \tag{7.14}$$

we get a continuum Lagrangian

$$\mathfrak{L}_B = \int d^d x \left(\psi_B^\star \frac{\partial \psi_B}{\partial \tau} + \frac{1}{2m} |\nabla \psi_B|^2 - \mu |\psi_B|^2 + \frac{1}{2} U |\psi_B|^4 \right) \tag{7.15}$$

At $T = 0$ this model has a quantum critical point at $\mu = 0$. For $\mu < 0$ the boson density vanishes, whereas a superfluid with finite boson density emerges for $\mu > 0$. Clearly, this transition is identical to any of the Mott–superfluid transition of the Bose-Hubbard model in Fig. 7.3 away from the tip of the Mott lobe (if an integer background density of bosons is added).

The field theory in Eq. (7.15) has dynamical exponent $z = 2$, and hence the upper critical dimension is $d_c^+ = 2$. For $d < 2$ boson self interactions are relevant at criticality,

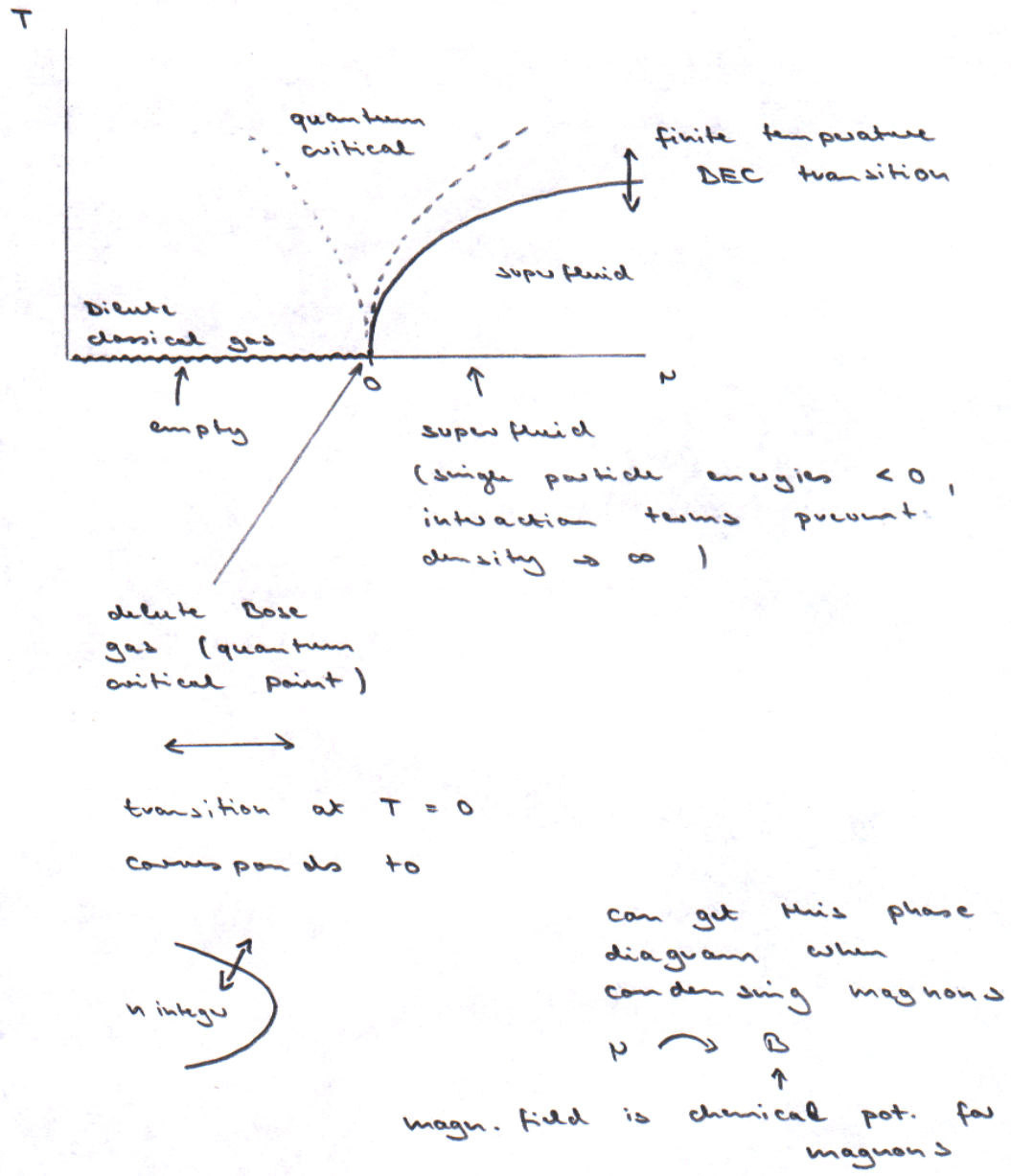

Figure 7.5: Phase diagram of the dilute Bose gas (in dimensions $d > 2$) as function of chemical potential μ and temperature T. The superfluid phase is bounded by a finite-temperature phase transition which ends at the QCP at $\mu = 0$, $T = 0$.

and the theory needs to be analyzed by RG techniques, see Sachdev's book [1] for details. Remarkably, for $d = 1$ the critical fixed point is identical to that of the dilute Fermi gas to be discussed below.

For $d > 2$ boson self interactions are irrelevant. Hence, mean-field theory applies but

the quartic interaction u is dangerously irrelevant and needs to be kept. The density obeys

$$\langle \psi_B^\star \psi_B \rangle = \begin{cases} 0 & \mu < 0 \\ \mu/u + \ldots & \mu > 0 \end{cases} \tag{7.16}$$

The finite-temperature crossovers are somewhat non-trivial: There is a dilute classical gas regime for $T < -\mu$ where the particle density is exponentially small. The high-temperature quantum critical regime is bounded by crossover lines $T \sim (|\mu|/u)^{2/3}$ in $d = 3$, and another crossover regime exists for $\mu < 0$. The phase diagram for $d = 3$ is sketched in figure 7.5.

We note a special property of the dilute Bose-gas model: (i) For $\mu < 0$, $T = 0$ the system is "empty", i.e., there are no particles and no fluctuations. This implies that there is no diverging correlation upon approaching the QCP at $T = 0$ from the negative-μ side. Nevertheless, the finite-temperature crossovers follow the standard quantum-critical phenomenology.

7.5 Dilute spinless Fermi gas

We finally turn to systems of fermions. The simplest situation is given by spinless non-interacting fermions – this is, of course, a textbook example of an exactly solvable model system. Focussing on the situation with the chemical located near the band bottom, the following discussion will cast well-known results into the scaling perspective of quantum phase transitions, and hence will be useful for a broader picture.

We consider a model of free fermions (defined either on a lattice or in the continuum)

$$H_F = \sum_k \frac{k^2}{2m} c_k^\dagger c_k - \sum_k \mu n_k \tag{7.17}$$

which is equivalent to the continuum Lagrangian

$$\mathfrak{L}_B = \int d^d x \left(\psi_F^\star \frac{\partial \psi_F}{\partial \tau} + \frac{1}{2m} |\nabla \psi_F|^2 - \mu |\psi_F|^2 \right) . \tag{7.18}$$

It can be shown that interactions (which must be non-local in space due to the Pauli principle) are irrelevant, hence are not written down – this is fundamentlly different from the dilute Bose gas discussed above.

At $T = 0$ the Fermi-gas model has a quantum critical point at $\mu = 0$ where the fermion density develops singular behavior:

$$\langle \psi_F^\star \psi_F \rangle = \begin{cases} 0 & \mu < 0 \\ (S_d/d)(2m\mu)^{d/2} & \mu > 0 \end{cases} \tag{7.19}$$

with $S_d = 2/[\Gamma(d/2) 4\pi^{d/2}]$. In other words, a quantum phase transition occurs upon tuning the chemical potential from zero to finite density of particles. In contrast to

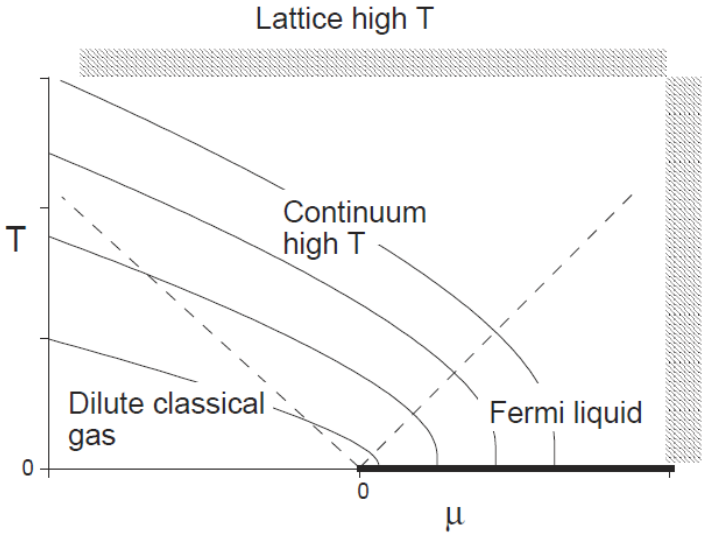

Figure 7.6: Phase diagram of the dilute Fermi gas as function of chemical potential μ and temperature T. The QCP determining the structure of the phase diagram is at $\mu = 0$, $T = 0$; it is the endpoint of a critical line located at $\mu > 0$, $T = 0$ which controls the Fermi-liquid phase. The dashed lines mark the crossover $T^* \propto |\mu|^{\nu z}$ with $\nu z = 1$; the solid lines denote lines of constant density. Figure taken from [1].

the case of bosons discussed in the previous section, the present QPT does *not* involve spontaneous symmetry breaking.[3]

Using standard thermodynamic relations, one can derive the free energy density which reads

$$\mathcal{F}_F = -T \int \frac{d^d k}{(2\pi)^d} \ln\left(1 + e^{(\mu - k^2/(2m))/T}\right) \tag{7.20}$$

which can be cast into the form

$$\mathcal{F}_F = T^{d/2+1} \Phi_{\mathcal{F}_F}\left(\frac{\mu}{T}\right) \tag{7.21}$$

where $\Phi_{\mathcal{F}_F}$ is a universal scaling function. Consequently, all thermodynamic observables show scaling behavior as function of μ/T. The quantum-critical regime must therefore be bounded by lines $\pm\mu \sim T$, i.e., $\nu z = 1$. The quadratic dispersion of the particles at $\mu = 0$ suggests $z = 2$, hence $\nu = 1/2$. Of course, these exponents also follow from a thorough scaling analysis [1].

The crossover phase diagram is shown in Fig. 7.6. The low-temperature regime for $\mu < 0$ is characterized by an exponentially small density of particles, hence their behavior is classical even in the (fixed-μ) low-temperature limit (recall that the thermal de-Broglie wavelength only diverges in a power-law fashion as $T \to 0$.) In contrast, in the high-temperature quantum critical regime both the inter-particle spacing and the thermal

[3]Sometimes the transition of the dilute Fermi gas is referred to as Lifshitz transition, because the topology of the Fermi surface changes (from non-existent to pocket-like).

de-Broglie wavelength scale as $1/\sqrt{T}$, such that quantum and thermal effects are equally important. Finally, the low-temperature regime for $\mu > 0$ is a standard finite-density Fermi gas (which turns into a Fermi liquid upon including interactions, except for $d = 1$ where it should be properly labelled Luttinger liquid).

As noted for the Bose gas, the $\mu < 0$, $T = 0$ state is fluctuationless. Further, the Fermi liquid itself can be understood as a critical system – it displays power-law correlations due to the presence of a Fermi surface - such that the $T = 0$, $\mu > 0$ line is a line of quantum critical points. Thanks to the linear dispersion near the Fermi surface, this critical line is characterized by a dynamical exponent $z = 1$ (as opposed to $z = 2$ at the $\mu = 0$ QCP).

7.6 Fermi-Hubbard Model

In this final section, we discuss the fermionic (=original) version of the Hubbard model, which reads

$$H = -t \sum_{\langle ij \rangle \sigma} (c^\dagger_{i\sigma} c_{j\sigma} + \text{h.c.}) - \mu \sum_{i\sigma} n_{i\sigma} + U \sum_i n_{i\uparrow} n_{i\downarrow} \tag{7.22}$$

for a single band of spin-1/2 fermions where $\sigma = \uparrow, \downarrow$ is a spin label. This model was proposed by Hubbard, Gutzwiller, and Kanamori in the 1960s, mainly as a model to describe the occurrence of ferromagnetism in materials with significant electron–electron interactions.

As for bosons, this model features an incompressible Mott-insulating phase at filling $n = 1$ (dubbed half filling), while $n = 0$ and $n = 2$ are commonly called band insulators. The compressible phase realized at small interactions or non-integer filling is a Fermi-liquid metal (which may be unstable to superconductivity, see below). A minimal phase diagram, similar to its bosonic counterpart, is sketched in figure 7.7.

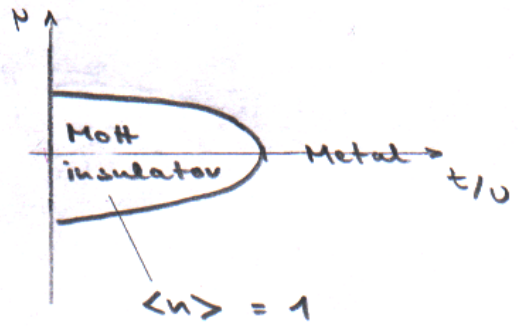

Figure 7.7: Simplified generic phase diagram of the Hubbard model. Symmetry-broken states (magnetic, superconducting, etc.) are not shown.

As compared to the Bose-Hubbard model discussed above, the main difference is (apart from the restricted local Hilbert space of fermions) the fact that fermions carry spin. As a result, the Mott insulator is *not* a trivial featureless phase, because spin

degrees of freedom (i.e. local moments) remain once the charges are frozen. As a result, magnetism plays a central role, which cannot only occur within the Mott-insulating phase, but also in the metal. Local moments and magnetic fluctuations can lead to a plethora of ordering phenomena, including the occurrence of high-temperature superconductivity. In fact, the one-band Hubbard model (7.22) is one of the simplest models which is believed to describe the physics of cuprate superconductors. However, many properties of this model are not understood to a sufficient degree to date, and continue to constitute an active area of current research.

7.6.1 Antiferromagnetism in the Mott insulator

To illustrate the emergence of magnetism, we consider the Mott-insulating phase in the limit of $U/t \gg 1$. In this regime $n = 1$ (with density fluctuations suppressed as $U/t \to \infty$), i.e., we have localized spins $\frac{1}{2}$ per lattice site.

Figure 7.8: Spin degrees of freedom at half filling.

For $U/t = \infty$ (or $t = 0$) particles are strictly immobile, hence all 2^N spin states are degenerate. Departing from this limit, virtual hopping processes like

$$\uparrow\downarrow \quad \Rightarrow \quad \cdot\updownarrow \quad \Rightarrow \quad \downarrow\uparrow \tag{7.23}$$

become possible for antiparallel spins on neighboring sites. These lead to an energy gain of order t^2/U. One can derive an effective model for the spin degrees of freedom valid for $t \ll U$ and $\langle n \rangle = 1$, which turns out to be an antiferromagnetic Heisenberg model:[4]

$$H = J \sum_{\langle ij \rangle} \left(\vec{S}_i \cdot \vec{S}_j - \frac{1}{4} \right) \tag{7.24}$$

with an antiferromagnetic exchange coupling $J = 4\frac{t^2}{U}$.

The Heisenberg model (7.24) displays an antiferromagnetic ground state on bipartite lattices, but can feature other types of phases (including spin liquids, valence-bond solids etc) on frustrated lattices.

[4]The Heisenberg form of the effective Hamiltonian is dictated by $\mathbb{SU}(2)$ symmetry.

7.6.2 Phases of the Hubbard model

The physics of the Hubbard model, both at and away from half-filling, is extremely rich and is not fully understood even for the square lattice.[11]

At half-filling where a metal is realized for small U/t (except for cases with perfect nesting of the Fermi surface) and an antiferromagnetic Mott insulator appears at large U/t, it is not a priori clear whether the phase boundary for antiferromagnetism and the one for the metal-insulator transition coincide on the U/t axis. While their coincidence may result in a simple first-order transition, a more interesting scenario seems to be realized on the triangular lattice, where a spin-liquid paramagnetic Mott insulator exists between the paramagnetic metal and the antiferromagnetic Mott insulator.

Away from half-filling, where the system is conducting, a plethora of symmetry-breaking phases have been discussed, and most research has been focussed on the square lattice believed to be relevant for the description of cuprate high-temperature superconductors. Most important is d-wave superconductivity which appears over a sizable range of dopings and interaction strengths U/t. Other possible phases include metallic charge and spin density waves as well as nematic states with broken lattice rotation but intact translation symmetries.

Bibliography

[1] S. Sachdev, *Quantum Phase Transitions (2nd ed.)*, Cambridge University Press (2011).

[2] N. Goldenfeld, *Lectures on Phase Transitions and the Renormalization Group*, Westview Press (1992).

[3] E. Fradkin, *Field Theories of Condensed Matter Physics (2nd ed.)*, Cambridge University Press (2013).

[4] L. Zhu, M. Garst, A. Rosch, and Q. Si, Phys. Rev. Lett **91**, 066404 (2003).

[5] D. Bitko, T. F. Rosenbaum, and G. Aeppli, Phys. Rev. Lett. **77**, 940 (1996).

[6] R. Coldea *et al.*, Science **327**, 177 (2010).

[7] Ch. Rüegg *et al.*, Nature **423**, 62 (2003).

[8] M. Jaime *et al.*, Phys. Rev. Lett. **93**, 087203 (2004).

[9] A. Kopp and S. Chakravarty, Nature Phys. **1**, 53 (2005).

[10] H. von Löhneysen, A. Rosch, M. Vojta, and P. Wölfle, Rev. Mod. Phys. **79**, 1015 (2007).

[11] P. A. Lee, Rep. Prog. Phys. **71**, 012501 (2008).